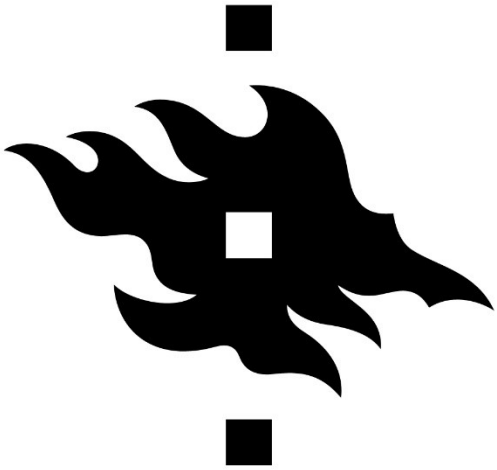

The Effect of Intrathecally Administered HB-GAM (Pleiotrophin) in the Cervical Hemisection and Cervical Hemicontusion Mouse Models of Spinal Cord Injury

Master's Thesis

Aino Lipponen

Master's Programme in Neuroscience (MNEURO)

Faculty of Biological and Environmental Sciences

University of Helsinki

May 2020

Supervisors: Heikki Rauvala and Natalia Kulesskaya

HELSINGIN YLIOPISTO
HELSINGFORS UNIVERSITET
UNIVERSITY OF HELSINKI

Tiedekunta – Fakultet – Faculty Biological and Environmental Sciences	Koulutusohjelma – Utbildningsprogram – Degree Programme Master's Programme in Neuroscience	
Tekijä – Författare – Author Aino Lipponen		
Työn nimi – Arbetets titel – Title The Effect of Intrathecally Administered HB-GAM (Pleiotrophin) in the Cervical Hemisection and Cervical Hemicontusion Mouse Models of Spinal Cord Injury		
Oppiaine/Opintosuunta – Läroämne/Studieinriktning – Subject/Study track Neuroscience		
Työn laji – Arbetets art – Level Master's Thesis	Aika – Datum – Month and year 05/2020	Sivumäärä – Sidoantal – Number of pages 50

Tiivistelmä – Referat – Abstract

Spinal cord injury (SCI) in human patients is the most expensive clinical condition worldwide, restricting individuals' ability to manage with daily-life activities independently. With very limited available treatment possibilities, the understanding and validating of regenerative mechanisms and treatment options in animal models is crucial for their translation to clinical practice. The majority of SCIs in human patients are contusive in the cervical level of the spinal cord. However, thoracic injury rodent model is more commonly studied, with only recent studies working with cervical contusion injury model. Chondroitin sulphate proteoglycans (CSPGs), and especially their CS chains, are thought to be the major inhibitory structures for neurite regeneration after SCI. However, current research has led to a new idea that the inhibitory effect of CS chains can be reversed to regeneration enhancing by heparin-binding growth-associated molecule (HB-GAM). This endogenously secreted molecule is highly up-regulated in the central nervous system (CNS) during postnatal development, but in the adult CNS the expression is down-regulated. This suggests that postnatal-level concentrations might be needed for inducing neurite regeneration in adult CNS. In this study, HB-GAM treatment was tested on both cervical hemicontusion and hemisection injury models. Here we show that repeated intrathecal injections of HB-GAM were sufficient to increase grey matter myelin optical density in mouse hemicontusion injury model, and partly induce functional recovery in hemisection model. Obtained anatomical evidence suggests that enhanced myelination is potentially involved in the repair mechanism of HB-GAM. The connection between HB-GAM treatment and functional recovery, and also other mechanisms of HB-GAM-induced regeneration need further exploration. In broader perspective, the results are promising for translation of a novel treatment approach to clinical use.

Avainsanat – Nyckelord – Keywords
Spinal cord injury, HB-GAM, pleiotrophin, chondroitin sulphate proteoglycans, animal model, cervical hemicontusion, cervical hemisection, intrathecal injection, myelin, chemical myelin gold chloride staining, glial scar.

Ohjaaja tai ohjaajat – Handledare – Supervisor or supervisors
Heikki Rauvala and Natalia Kulesskaya

Säilytyspaikka – Förvaringställe – Where deposited

Muita tietoja – Övriga uppgifter – Additional information

HELSINGIN YLIOPISTO
HELSINGFORS UNIVERSITET
UNIVERSITY OF HELSINKI

Tiedekunta – Fakultet – Faculty Bio- ja ympäristötieteellinen tiedekunta	Koulutusohjelma – Utbildningsprogram – Degree Programme Neurotieteen maisteriohjelma	
Tekijä – Författare – Author Aino Lipponen		
Työn nimi – Arbetets titel – Title Intratekaalisen HB-GAM-/pleiotrofiinilääkityksen vaikutus kaularangan hemisektio- ja kontuusioselkäydinvauriohiirimalleissa		
Oppiaine/Opintosuunta – Läroämne/Studieinriktning – Subject/Study track Neurotiede		
Työn laji – Arbetets art – Level Maisterintutkielma	Aika – Datum – Month and year 05/2020	Sivumäärä – Sidoantal – Number of pages 50

Tiivistelmä – Referat – Abstract

Selkäydinvauriot ovat maailmanlaajuisesti kalleimpia kliinisesti hoidettavia sairauksia, ja ne rajoittavat potilaan kykyä selviytyä itsenäisesti jokapäiväisistä aktiviteeteista. Saatavilla olevia hoitomuotoja on hyvin rajoitetusti, joten eläinmalleilla tehtävä tutkimus regeneratiivisten mekanismien ja hoitovaihtoehtojen ymmärtämiseksi ja validoimiseksi on ehdottoman tärkeää, jotta niitä voitaisiin soveltaa kliinisessä työssä. Suurin osa ihmisillä tapahtuvista selkäydinvaurioista on kontuusioita, kohdistuen selkäytimen kaularangan alueelle. Tästä huolimatta suurin osa tutkimuksesta on tehty jyrsijämalleilla, joille on indusoitu rintakehän alueen selkäydinvaurio, ja vain muutamat tutkimukset käsittelevät kaularangan alueen kontuusiomalleja. Kondroitiinisulfaattiproteoglykaanien (KSPG) ja erityisesti niiden kondroitiinisulfaattiketjujen (KS-ketjut) uskotaan olevan pääasiallisia hermosolukontaktien regeneraatiota estäviä rakenteita selkäydinvaurion jälkeen. Viimeaikainen tutkimus on kuitenkin johtanut uuteen ideaan, jossa KS-ketjujen regeneraatiota estävä vaikutus on mahdollista muuttaa edistäväksi vaikutukseksi hyödyntämällä hepariiniin ja KS-ketjuihin sitoutuvaa kasvuun assosioituvaa molekyyliä (heparin-binding growth-associated molecule, HB-GAM), jonka tiedetään edistävän regeneraatiota. HB-GAM on endogeenisesti erittyvä molekyyli, ja sen ilmentyminen on voimakasta keskushermostossa syntymänjälkeisen kehityksen aikana, toisin kuin aikuisilla, joiden keskushermostossa ilmentyminen on paljon vähäisempää. Tämä voi viitata siihen, että aikuisilla regeneraation indusoiminen vaatii samanlaista HB-GAM-konsentraatiota, joka vallitsee syntymänjälkeisessä vaiheessa. Tässä tutkimuksessa HB-GAM-lääkitystä testattiin kahdella kaularangan alueen selkäydinvauriohiirimallilla, hemikontuusiolla ja hemisektiolla. Tutkimustulokset osoittivat, että toistettu intratekaalinen HB-GAM-injektiohoito oli riittävä lisäämään harmaan aineen myeliinin optista tiheyttä hemikontuusiomallilla, ja toiminnallisen tason osittaista toipumista hemisektiomallilla. Osoitetut tulokset anatomisella tasolla viittaavat siihen, että lisääntynyt myelinisaatio voi liittyä HB-GAMin korjausmekanismeihin. Muut korjausmekanismit saattavat liittyä HB-GAMin aksonien regeneraatiota edistävään vaikutukseen, mutta ne, sekä HB-GAM-hoidon ja toiminnallisen tason toipumisen välinen yhteys vaativat vielä lisää tutkimusta. Tutkimustulokset osoittavat HB-GAMin olevan lupaava hoitovaihtoehto, jolla voi olla sovellusmahdollisuuksia kliinisessä käytössä.

Avainsanat – Nyckelord – Keywords
Selkäydinvaurio, HB-GAM, pleiotrofiini, kondroitiinisulfaattiproteoglykaanit, eläinmalli, kaularangan alueen hemikontuusio, kaularangan alueen hemisektio, intratekaalinen injektio, myeliini, kemiallinen myeliinikultakloridivärjäys, glia-arpi.

Ohjaaja tai ohjaajat – Handledare – Supervisor or supervisors Heikki Rauvala ja Natalia Kulesskaya
Säilytyspaikka – Förvaringställe – Where deposited
Muita tietoja – Övriga uppgifter – Additional information

Table of Contents

Abbreviations

BL	Baseline
BSCB	Blood-spinal cord barrier
ChACB	Chondroitinase ABC
CNS	Central nervous system
CSPG	Chondroitin sulphate proteoglycan
CS side chain	Chondroitin sulphate side chain
DAMP	Danger-associated molecular pattern
ECM	Extracellular matrix
GAG side chain	Glycosaminoglycan side chain
GFAP	Glial fibrillary acidic protein
GPI linker	Glycosylphosphatidylinositol linker
HB-GAM	Heparin-binding growth-associated molecule
HS proteoglycan	Heparan sulphate proteoglycan
MBP	Myelin basic protein
MS	Multiple sclerosis
OPC	Oligodendrocyte precursor cell
PNS	Peripheral nervous system
PTPσ	Protein tyrosine phosphatase sigma
ROCK pathway	Rho-associated kinase pathway
SCI	Spinal cord injury

1. Introduction

1.1 Spinal Cord Injury (SCI)

1.1.1 General Information: Prevalence, Injury Types, and Current Treatment Options

Spinal cord injury (SCI) is defined as a damage to the spinal cord caused by a trauma instead of a disease. The biggest prevalence is in USA (906 per million), and the lowest in the Rhone-Alpes region, France (250 per million), and in Helsinki, Finland (280 per million) (Singh *et al.*, 2014). Annually, approximately 17 000 new cases of SCI are recorded in North America (NSCISC, 2018), with the annual total cost of approximately $9.7 billion (Berkowitz *et al.*, 1998), and approximately 250 000 to 500 000 individuals world-wide (World Health Organization, 2019). The symptoms of SCI may include partial or complete loss of sensory and/or motor functions of arms, legs and/or body, and the most severe cases cause problems with breathing, heart rate, blood pressure, and bowel or bladder control (incontinence). In addition, most SCI patients experience chronic pain. The severity and extent of the symptoms depend on the injury type, severity, and the location of the injury (World Health Organization, 2019). Current treatment options for SCI involve acute surgical procedures aiming to decompress and stabilize the spinal cord immediately after the injury, and long-term treatments, which involve pain controlling and psychological and physical therapy, focusing on managing the symptoms arising from maladaptive plasticity and other secondary complications (see in Tran, Warren and Silver, 2018). The effectiveness of the treatment options is very limited, varying between individuals and depending on the severity of trauma and the location of the injury. Due to these features, SCI is considered to be the most expensive chronic medical condition (NSCISC, 2018), and with very limited available treatment options, the validation of animal models of SCI is very crucial for development, testing and translation of the novel treatment strategies to clinical use.

1.1.2 Animal Models of SCI

In general, animal models are a valuable tool for SCI research, enabling the discovery of the factors regulating, inhibiting and enhancing recovery of the injury at multiple levels, and the preclinical testing of novel treatment candidates. Mouse (Mus musculus) is the commonly used animal model due to its multiple beneficial features, including the transgenic technology developed for mouse, a high variety of available strains, fast reproduction, cost-effectiveness, and as a mammal, enough similar genome compared to humans (Vandamme, 2014; Sharif-Alhoseini *et al.*, 2017). There are also multiple other experimental animal species commonly used, including rats, cats, dogs and swine. Usually the housing price and requirements of bigger experimental animals limits the sample size critically, which also in part leads to the favouring of rodents in research.

More than a half of the reported cases of human SCIs occur at the cervical level of the spinal cord, which leads to complete or incomplete tetraplegia (NSCISC, 2018). The regaining of arm and hand function is the top priority for most tetraplegic individuals (Anderson, 2004), and hence there is a need for evaluating therapy approaches using cervical injury models, with forelimb function recovery used as an outcome measure (Streijger *et al.*, 2013). Many SCI studies in rodents are produced at the thoracic level of spinal cord, and only few use a more clinically relevant cervical model (Anderson, Abdul and Steward, 2004; Duffy *et al.*, 2009). This is problematic since the findings of thoracic experiments are not directly translatable to cervical level injuries (Streijger *et al.*, 2013). The differences between spinal cord levels include size and vascularisation. Moreover, the different levels of the spinal cord involve descending (motor) and ascending (sensory) nerve tracts from different CNS and PNS areas. Hence, the affected sensory and motor nerve tracts differ between the spinal cord levels injured. Due to these differences, a promising treatment candidate or rehabilitation procedure for injury at each level must be tested at the other ones as well.

1.1.2.1 Lateral Hemisection SCI Model

Lateral hemisection SCI model in mice is done by a cut on the spinal cord area of interest, and it mimics the Brown-Sequard syndrome in humans, which is a rare condition caused most often by a penetrating injury to the spinal cord. The disease is characterized by ipsilateral loss of motor function, proprioception, and vibratory sense, and contralateral loss of both pain and temperature sensitivity (Tattersall and Turner, 2000). Cervical hemisection animal model is beneficial since it significantly reduces the need for chronic intensive care after SCI in comparison with bilateral cervical contusion injury in mice (Aguilar and Steward, 2009), but still provides a reliable model for SCI experiments. The main advantage of this model is the accuracy of trauma cut that allows to study axonal regeneration of the precise area in laboratory conditions (Sharif-Alhoseini *et al.*, 2017). However, the model reflects only a small percentage of human SCIs, and the regeneration-inducing treatments tested in a transection model should also be tested and optimized in a contusion model, and vice versa, because of the different features of the injury models (Vogelaar and Estrada, 2016).

1.1.2.2 Lateral Hemicontusion SCI Model

Lateral hemicontusion trauma model is generated by applying a controlled pressure with defined force and/or velocity on the spinal cord after laminectomy (Geissler, 2013). There are multiple commercially available systems for inflicting standardized graded contusion models, including the Infinite Horizon (IH) impactor (Lee *et al.*, 2012) that was used in this experiment. The contusion injury model is the most relevant model for clinical practice, since with blunt

compression injury model it mimics well the neuropathology in human SCIs (Kwon, Oxland and Tetzlaff, 2002; Gensel *et al.*, 2006; Kwon, Hillyer and Tetzlaff, 2010). Compared to transection model, however, the contusion model is more challenging to produce, since it is difficult to evaluate how big and severe the trauma will be even when the compression is done automatically. In addition, there are always some spared fibers after the injury, which complicates the defining of actual regenerating fibers from the spared ones (Vogelaar and Estrada, 2016).

1.2 SCI: Tissue and Cellular Level

SCIs are evoked due to a physical trauma, followed by tissue remodelling that can be described as primary and secondary injuries, and the formation and maturation of the glial scar. Physical trauma is typically brief, but the subsequent tissue remodelling can persist for a very long time, peaking weeks after injury. It induces glial and neural necrosis at the lesion epicenter, which expands symmetrically (Grossman, Rosenberg and Wrathall, 2001), and contributes to the inflammatory milieu of the injury site. Apoptosis also happens after physical trauma, including longer-lasting glial apoptosis and shorter lasting neuronal apoptosis (Citron *et al.*, 2000). Along the lesion area, there is shearing and degeneration of both descending and ascending axons (Muradov, Ewan and Hagg, 2013). In addition, aggressive macrophage activity (Kigerl *et al.*, 2009; Cherry, Olschowka and O'Banion, 2014) and demyelination of axons (Bresnahan, 1978) contribute to axonal dieback (Busch *et al.*, 2009).

1.2.1 Primary Injury

Primary injury is the first phase after physical trauma in the spinal cord, beginning with trauma-caused vascular disruption, leading to rupturing of blood-spinal cord barrier (BSCB). Edema with homeostatic imbalance follows the breakdown of BSCB due to unfettered flow of ions and water, and further haemorrhage occurs especially in the grey matter due to blood vessel rupture of BSCB (Tran, Warren and Silver, 2018). Bleeding causes cavitation of the lesion site and further expansion of the injury area due to compression along the cord. Ischemia in grey matter follows haemorrhage staunching responses, and it includes vasospasm and constriction of blood vessels (Sandler and Tator, 1976). Furthermore, ischemia leads to oxidative stress and glial apoptosis 3 hours post-injury at the lesion epicenter (Muradov, Ewan and Hagg, 2013). Neuronal excitotoxicity is also a part of the primary injury, which is due to the increase of released ions at the lesion site. The repair of BSCB basal lamina is incomplete due to the loss of lesion core astrocytes, which leads to abnormal profuse vasculature at the lesion area and the formation of a lesion cavity after resorption. Importantly, the breakdown of the BSCB during the primary injury with accompanying leakage of blood and serum elements into the serum parenchyma is a key event in glial scar formation (Cregg *et al.*, 2014).

1.2.2 Secondary Injury

Secondary injury includes a complex cascade of inflammatory factors, and it lasts for weeks, until the wounds are sealed, and the glial scar maturates. During the secondary injury, tissue damage expands from the lesion epicenter, including inflammation-induced apoptosis of adjacent cells and axotomy of spared neurons (Fitch *et al.*, 1999). Danger-associated molecular patterns (DAMPs) are in a key role participating inflammation during secondary injury. DAMPs are released from necrotic or apoptotic cells, and include for example alarmins, which participate in sterile inflammatory response in CNS (Bianchi, 2007).

Driven by the activation of microglia and macrophages, secondary injury eventually results in increased vascular permeability and accumulation of inflammatory cells in the lesion area.

Microglia has a beneficial role at the lesion center removing debris (Greenhalgh and David, 2014), which is especially important due to the apoptosis of oligodendrocytes and neurons (Liu *et al.*, 1997). The M2-like phenotype of microglia, dominating during normal brain functions (Cherry, Olschowka and O'Banion, 2014), is suddenly changed after injury to an amoeboid shape (Wu *et al.*, 2005), the M1-like phenotype, and the cells migrate to the lesion area in response to alarmins (Gadani *et al.*, 2015). There is a high concentration of microglia at the lesion core early after the injury (Greenhalgh and David, 2014), followed by migration to the marginal region (Evans *et al.*, 2014).

After BSCB damage, leukocytes including neutrophils, monocytes, and macrophages undergo extravasation, a series of stereotyped processes, including rolling adhesion and transmigration through BSCB, continuing towards the chemoattractant source (Trivedi, Olivas and Noble-Haeusslein, 2006; Stirling *et al.*, 2009). Neutrophils are the first ones of peripheral immune cells infiltrating in the injury site after injury (Chatzipanteli *et al.*, 2000), with a short-lasting presence (Fleming *et al.*, 2006). At the lesion site, they activate other immune and glial cells and hence potentiate inflammatory cascade (Chatzipanteli *et al.*, 2000).

Monocytes are also extravasating and differentiating into activated macrophages in the injured spinal cord (Kigerl *et al.*, 2009). These M1-activated macrophages dominate early lesion site (Kigerl *et al.*, 2009) and initiate secondary damage by secreting enzymes and proinflammatory factors, and also potentiate apoptosis (Kawabata *et al.*, 2010).

Macrophages are recruited to the lesion core and margins (Shechter *et al.*, 2009), with M1 as the most dominant phenotype at the lesion (Kigerl *et al.*, 2009). Their key tasks include phagocytising cellular debris and degenerating tissue remains (Greenhalgh and David, 2014), and by making intimate contacts with dystrophic ends of axons, they promote axonal retraction or dieback. In that way, activated macrophages are participating the regeneration failure at the lesion core (Tran, Warren and Silver, 2018).

Dieback or retraction of injured axons happens when axon tips move away from the injury site. It has two distinct phases: acute dieback occurs via intracellular Ca^{2+}-dependent cysteine proteases, leading to the formation of either an endbulb or a growth cone (Hill, 2017). This phase is followed by a more prolonged one, the protracted axonal dieback, when axonal endings withdraw progressively from the injury site. The key factors of the protracted dieback include the interaction of inflammatory cells, especially activated macrophages (Horn *et al.*, 2008; Hill, 2017). Macrophages are in a key role mediating the protracted dieback via matrix metalloprotease (MMP) enzyme activity and direct physical interaction with injured axons (Horn *et al.*, 2008). Dieback is terminated when dystrophic tips of axons make synaptic-like contacts with NG2+ oligodendrocyte progenitor cells, which stabilizes the retraction bulb structures (Tran, Warren and Silver, 2018).

1.2.3 Chronic Trauma and Glial Scar Formation

The chronic stage of SCI follows secondary injury, leading to a chronic failure of axonal regeneration, lasting for a lifetime. Glial scar is an important structure in the chronic stage, serving as a chronic physical and molecular barrier entrapping dystrophic axons and limiting their regenerative ability over long distances after SCI (Cregg *et al.*, 2014). A traditional view included the idea that the scar is a major barrier for axonal regeneration along the lesion site, trying to reach their distal targets, but it is now realised that the lesion consists of multiple interacting cell types, forming a complex entity (Horn *et al.*, 2008; Göritz *et al.*, 2011; Soderblom *et al.*, 2013). These interacting cells form a mature lesion that consists of the penumbra and the lesion core. The glial component of the scar includes reactive astrocytes, $NG2^{+}$ oligodendrocyte precursors, and microglia in the lesion penumbra, whereas the fibrotic component of the lesion center is created due to persistent low-grade inflammation and subsequent gliosis, with the extracellular matrix (ECM) remodelled with the increase of fibronectin, collagen, and laminin (Tran, Warren and Silver, 2018).

1.2.3.1 Astrocytes

After SCI happens reactive astrocytosis, which is part of the post-injury astroglial response. Reactive astrocytosis consists of upregulation of intermediate filament decorating proteins glial fibrillary acidic protein (GFAP) and vimentin (Xu *et al.*, 1999), hypertrophy of the primary branches (Sun *et al.*, 2010), and expansion of normally defined astrocytic domains at the injury site (Wanner *et al.*, 2013), with very restricted proliferation (Wanner *et al.*, 2013). Astrocytes migrate away from the lesion epicenter to the lesion penumbra, producing a thin layer (Faulkner *et al.*, 2004). The primary role of the thin layer is to restrict inflammation to the lesion epicenter and prevent further damage of the surrounding intact neural networks (Faulkner *et al.*, 2004; Wanner *et al.*, 2013). However, the major physical barrier to regenerating axons is produced by astrocytic hypertrophy, when astrocytes swell in size and create palisading-like patterns with

thick hypertrophied processes densely overlapping and packing around the lesion (Wanner *et al.*, 2013). Especially the upregulation of GFAP helps to allow the formation of the densely bundled structure around the lesion (Xu *et al.*, 2015). Importantly, astrocytes synthesize neurite regeneration inhibitory chondroitin sulphate proteoglycans (CSPGs) in the ECM within 24 hours post-injury, resulting in a high concentration of CSPGs that can persist for weeks to months (Jones, Margolis and Tuszynski, 2003).

Reactive astrogliosis, the proliferation of astrocytes, also happens after injury. It typically occurs in the inner margin of the lesion penumbra, directly next to the inflammatory core. Reactive astrocytes derive from ependymal cells (Meletis *et al.*, 2008), NG2+ OPCs (Zhu, Hill and Nishiyama, 2008), but mostly from other reactive astrocytes (Göritz *et al.*, 2011).

1.2.3.2 Oligodendrocytes

During non-injured conditions of the CNS, the pre-progenitor and immature states of oligodendrocytes transiently express axonal growth inhibitory CSPG, NG2, followed by possessing the ability to myelinate (Baumann and Pham-Dinh, 2001). However, a physical impact to spinal cord leads to the apoptosis of both mature and immature oligodendrocytes (Liu *et al.*, 1997), followed by depletion of oligodendrocytes both rostral and caudal sides along degenerating axon tracts during the secondary injury that lasts for weeks (Li, Field and Raisman, 1999). $NG2^+$ oligodendrocyte progenitor cells (OPCs) proliferate following injury (Lytle *et al.*, 2009) and accumulate in the lesion epicenter and penumbra (McTigue, Wei and Stokes, 2001; Lytle *et al.*, 2009). During secondary injury, OPCs become reactive, leading to increased expression of NG2. In addition, activated $NG2^+$ oligodendrocytes change their morphology, accumulating into dense plaques surrounding the lesion site. Furthermore, $NG2^+$ glia participates in activation of macrophages and astrocytes (Rodriguez *et al.*, 2014), contributing to the inflammatory milieu of the lesion (Kucharova and Stallcup, 2015).

The continued growth of axons is prevented by the inhibitory scar, and they form dystrophic growth cones with bulbous morphology. Recent research has revealed that dystrophic growth cones are more active than previously thought (Tom *et al.*, 2004), and chronically injured axons retain their potential to regenerate when provided with optimal cues (Kwon, Oxland and Tetzlaff, 2002). In vivo findings indicate that disorganized microtubules are in a key role in the formation of the dystrophic growth cones (Ertürk *et al.*, 2007). Interestingly, $NG2^+$ glial cells highly colocalize with dystrophic axonal growth cones (Nishiyama *et al.*, 2002; Jones, Margolis and Tuszynski, 2003; McTigue, Tripathi and Wei, 2006), and make stable contacts which prevents axonal dieback caused by inflammatory cells. This interaction leads to the formation of synaptic-like interactions between the NG2 glia and axons, also called “synaptoids”, further stabilizing severed axon tips along the lesion penumbra, but also constraining the axonal regeneration

(Filous *et al.*, 2014). A human case study has shown that some dystrophic growth cones persist for 40 years, suggesting that they might last indefinitely (Tran, Warren and Silver, 2018).

In addition to NG2, other CSPGs of the astroglial scar including versican and neurocan are potently causing inhibition of oligodendrocyte myelination (Pendleton *et al.*, 2013), probably contributing to the chronic remyelination failure following SCI (see in Tran, Warren and Silver, 2018). In a more detailed view, OPCs express receptor protein tyrosine phosphatase sigma (PTPσ), which in the presence of CSPGs leads to inhibition of vital oligodendrocyte functions including proliferation, differentiation, migration, and myelination through downstream Rho-associated kinase (ROCK) pathway and Rho signalling (Pendleton *et al.*, 2013). In addition, remyelination failure is also caused by CSPG-driven inhibition of OPCs differentiation into mature, myelinating state (Karus *et al.*, 2016). Remyelination is often incomplete (Keirstead, Levine and Blakemore, 1998), which leads to long-term functional deficits of spared axons. Furthermore, demyelination of spared axons on near and distant sites of injury makes them dysfunctional (Nashmi and Fehlings, 2001) and more susceptible to injuries (see in Pendleton *et al.*, 2013).

In their study, Pendleton et al. (2013) demonstrated that by removing the glycosaminoglycan (GAG) side chains of CSPGs via chondroitinase ABC (ChABC) enzymatic degradation, CSPG inhibitory effect of oligodendrocyte process outgrowth and myelination was reversed. The results indicate that the CSPG-driven inhibitory effect of axon myelination process of oligodendrocytes is dependent on intact GAG side chains. They also showed that RNAi-mediated down-regulation of PTPσ, a receptor that partly mediates CSPG inhibitory effect, was sufficient to reverse the inhibitory effect. Furthermore, a downstream pathway of PTPσ, ROCK pathway, which partially mediates the axonal regeneration inhibitory properties of CSPGs, was shown to participate also in the oligodendrocyte process outgrowth and myelination inhibition (Pendleton *et al.*, 2013). ROCK pathway has been suggested to be a candidate therapeutic target of CNS injuries in both neuron and glial level.

1.2.3.3 Fibroblasts

During the maturation of the glial scar, meningeal or perivascular fibroblasts migrate to the lesion site, proliferate and participate in the formation of a fibrotic scar in the lesion epicenter (Cregg *et al.*, 2014).The fibrotic core maturates 2 weeks post-injury (Göritz *et al.*, 2011; Soderblom *et al.*, 2013). Fibrotic scar is important in the acute healing process after injury, participating to the contraction of the lesion and wound closure. However, meningeal fibroblasts express repulsive axon guidance molecules (Pasterkamp *et al.*, 1999) and promote astrocytic reactivity (Wanner *et al.*, 2008), hence contributing to the axon regeneration inhibitory properties of the scar. Pericytes also contribute to the fibrotic scar by delaminating from the basal laminae

of the lesion-surrounding blood vessels and migrating to the lesion core and chronically differentiating into fibroblast-like cells (Göritz *et al.*, 2011; Soderblom *et al.*, 2013).

1.3 CSPGs: Chondroitin Sulphate Proteoglycans

Chondroitin sulphate proteoglycans (CSPGs) are ECM proteins including neurocan, aggrecan, brevican, phosphacan, versican, and NG2 (Margolis and Margolis, 1993). All chondroitin sulphate (CS) GAG side chains are covalently linked to different protein cores (Kwok *et al.*, 2011) and the number, length and pattern of the sulphation of the side chains are produced during posttranslational modifications of the CSPGs (Margolis and Margolis, 1993).

It's generally accepted that CSPGs act as major inhibitors of plasticity and regeneration in the adult CNS, and the CS chains are the major inhibitory structures of the CSPGs (Rauvala *et al.*, 2017). The developmental role of proteoglycans in the CNS is the formation of boundaries via preventing growing neurons from spreading to sites at which they are already enriched (Snow *et al.*, 1990), and that fits well with their importance in post-injury neurite growth inhibition. In addition, CSPGs inhibit axonal growth in culture (Snow *et al.*, 1990).

In mature mammals, CSPGs are secreted rapidly, within 24 hours, after CNS injury and can persist for months. Almost all cell types at the injury site participate in the secretion, especially astrocytes (Tang, Davies and Davies, 2003). CSPGs accumulate in the glial scar after CNS injury, and it is thought to be the main area for exerting the inhibitory effect of CS chains. The proteoglycan gradient is highest in the lesion center, diminishing gradually into the penumbra (Rolls, Shechter and Schwartz, 2009). This increasingly inhibitory CSPG-rich area prevents neurites approaching the lesion center, even though some neuron types have better ability to regenerate in the inhibitory environment than others (Inman and Steward, 2003). Nevertheless, all growing fibers eventually succumb and develop dystrophic endings while approaching the CSPG-rich area (Silver and Miller, 2004).

The mechanistic explanation of how CSPGs inhibit advancing growth cones suggests the binding of CS chains with multiple receptors, especially the inhibitory cell surface receptor PTPσ. Binding of CSPGs and PTPσ results in axonal growth inhibition (Shen *et al.*, 2009). To support this explanation, it has been shown that PTPσ knockout mice have increased axonal regeneration after corticospinal tract injury (Fry *et al.*, 2009).

Removal of CSPG CS chains via ChABC enzymatic digestion has been shown to result in regeneration and functional recovery after SCI (Bradbury *et al.*, 2002). The enzyme selectively removes a large portion of the CSPG GAG side chain, leaving the protein core and stub carbohydrate. In addition, CSPG digestion with ChABC treatment has been shown to improve regeneration after spinal cord hemisection of a cat and after a compressive injury of the spinal cord in rats (Silver and Miller, 2004).

Despite of the promising results of CSPG digestion, there are some limitations of ChABC treatment. For example, an in vitro study showed that after ChABC treatment, remaining CSPG protein core and sugar stub still remain somewhat inhibitory to adult dorsal root ganglion process outgrowth (Silver and Miller, 2004). In addition, an in vivo study included the pre-digestion of aggrecan with chondroitinase, but surprisingly, the addition of purified protein core in spinal cord led still to regeneration inhibition (Lemons *et al.*, 2003). It can be hence concluded that ChABC treatment does not remove all inhibitory aspects of CSPGs, and different ways of manipulating CSPGs are needed as well.

CSPGs have also beneficial effects in the lesion area, including modulating immune responses and restricting them to the damaged area, and regulating progenitor cell proliferation (Rolls, Shechter and Schwartz, 2009). In addition, CSPGs also act as a diffusion barrier for molecules potentially harmful to spared tissue (Roitbak and Syková, 1999), attenuating the spread of neurotoxicity (Voříšek *et al.*, 2002), and preventing excitatory amino acid-induced neuron death (Sato *et al.*, 2008). Therefore, there is a need for developing alternative approaches for CSPGs degrading treatments, without destroying the biologically important structures.

1.4 HB-GAM

Heparin-binding growth-associated molecule (HB-GAM), also called as pleiotrophin (PTN), was originally isolated by screening factors from rat brain extracts that enhance neurite outgrowth in CNS neurons (Rauvala, 1989). It is known to enhance neurite extension in CNS neurons as a substrate-bound molecule, and it is a glycosaminoglycan-binding protein (Rauvala, 1989; Li *et al.*, 1990; Merenmies and Rauvala, 1990; Raulo *et al.*, 1992). HB-GAM is secreted from neurons and glial cells via a classic-type secretion signal mechanism (Milev *et al.*, 1998; Sugahara and Mikami, 2007).

During the first weeks of postnatal development the expression level of HB-GAM is very high, with the peak during postnatal developmental weeks 3-4 in rat brain (Merenmies and Rauvala, 1990), 10–15 µg/g of wet tissue weight (Rauvala, 1989). In addition, HB-GAM widely lines fiber tracts of the early postnatal rat brain (Rauvala *et al.*, 1994), enhances synaptogenesis, and participates in the regulation of neuronal migration in developing brain (Rauvala *et al.*, 1994, 2000). In the adult CNS, HB-GAM expression is strongly downregulated, which correlates with the decreased plasticity of the adult CNS compared to juvenile (Hensch, 2004), suggesting that the expression level in the juvenile brain is probably sufficient to modulate neural plasticity and regeneration inhibiting matrix structures (Milev *et al.*, 1998).

1.4.1 HB-GAM Expression after CNS Injuries

HB-GAM or PTN mRNA and protein expression has been shown to change after multiple types of CNS injuries. Yeh et al. (1998) showed that after acute ischemic brain injury, there was

upregulation of *Ptn* in OX42-positive macrophages, astrocytes, and endothelial cells in areas of developing neovasculature within 3 days, remaining upregulated for 7 to 14 days post-injury. There was a significant decrease of *Ptn* expression in degenerating cortical neurons for 6 to 24 hours post-injury, and it was undetectable at day 3. This may suggest that the absence of *Ptn* expression in neurons may contribute to their failure to survive. Yeh et al (1998) also showed PTN protein expression in the microvasculature and macrophages of the area of infarct, and on day 7, there were large numbers of PTN-positive macrophages and hyperplastic blood vessels in the injured area.

A study of Takeda et al. (1995) used two types of neuronal injuries, transient forebrain ischemia in the hippocampal CA1 area, and an intraventricular kainate injection, which causes selective pyramidal cell necrosis in the CA3 region. Both injury types induced HB-GAM mRNA expression on day 4 post-injury in reactive astrocytes, followed by HB-GAM protein induction on day 7. This indicates a corresponding increase of HB-GAM protein expression in the surrounding ECM caused by upregulation of HB-GAM mRNA expression. Surprisingly, they detected no HB-GAM protein in cortical neurons despite of corresponding mRNA expression.

To take into account SCIs, a study by Wang et al. (2004) showed that after spinal cord transection, HB-GAM mRNA was upregulated on both rostral and caudal side of the lesion, starting 3 days post-injury, peaking at day 7, with higher upregulation on the rostral side. HB-GAM protein expression was increased at day 7 post-injury and was co-localized with astrocytes, oligodendrocytes, and neurons in spinal cord tissue close to the lesion site.

These studies show that HB-GAM or pleiotrophin (PTN) mRNA and protein expression is altered after different types of brain and spinal cord injuries. The results may suggest that the expression of HB-GAM in neurons post-injury might be an intrinsic reparative mechanism aiming at promoting injured axons to regenerate.

1.4.2 HB-GAM and CSPGs

CSPGs have been seen mostly as neurite regeneration and plasticity inhibiting factors in adult CNS (Rauvala *et al.*, 2017), but recent research has raised a new idea that the neurite outgrowth inhibitory effect of CSPGs can be reversed to an enhancing one via HB-GAM treatment. There is a lot of research providing supportive evidence for this idea, but the actual mechanism of how the interaction between HB-GAM and CSPGs may contribute to the enhancing effect has been studied in more detail only recently.

HB-GAM binds to CS chains of CSPGs at nanomolar Kd values (Milev *et al.*, 1998; Sugahara and Mikami, 2007). HB-GAM has a dual structure with C-terminal and N-terminal domains connected with a flexible linker, and the binding sites for GAGs are placed on both C- and N-terminal regions (Kilpeläinen *et al.*, 2000). The binding effect between HB-GAM and CS chains

has been observed on multiple CSPG substrates in vitro, including aggrecan, neurocan and a CSPG mixture from brain (Paveliev *et al.*, 2016). In addition, removal of CS chains via ChABC digestion reduced the inhibitory effect of substrate-bound aggrecan on neurite outgrowth, but it also abolished the promoting effect of neurite outgrowth with HB-GAM treatment (Paveliev *et al.*, 2016). This finding suggests that CS chains and the formation of HB-GAM/CS complex are essential for the neurite outgrowth promoting effect.

An idea proposed by Rauvala et al. (2017) suggests that HB-GAM acting as regeneration promoting factor is due to its masking of CS chain binding sites of PTPσ. After being secreted to the ECM, HB-GAM binds to CS chains of substrate-bound CSPGs and masks the binding sites of PTPσ, a neurite outgrowth inhibitory transmembrane receptor (Lang *et al.*, 2015), enabling the matrix to become more permissive for neural regeneration. Paveliev et al. (2016) showed that there is a competition between PTPσ and HB-GAM in the aggrecan CS chain binding, by demonstrating the HB-GAM dose-dependent inhibition of PTPσ binding to substrate-bound aggrecan. HB-GAM was also shown to bind to CS chains of aggrecan but not to PTPσ. Interestingly, the knockdown of PTPσ in CNS neurons had no neurite outgrowth inducing effect on CSPG substrate with or without added HB-GAM, indicating that the downregulation of PTPσ is not alone sufficient to explain the neurite outgrowth-promoting effect of HB-GAM, even though it probably participates enhancing the permissiveness of CSPG matrix for neurite outgrowth (Rauvala *et al.*, 2017).

Since CSPGs have inhibitory effects on axonal regeneration via glial scar and oligodendrocyte process outgrowth and myelination, it can be hypothesized that HB-GAM could be a possible treatment candidate reversing these inhibitory effects. As described earlier in the text, CSPGs are biologically important structures, and the removal of GAG chains might have multiple harmful effects. The loss of GAG chains could be avoided with HB-GAM treatment, since there is a competition between HB-GAM and PTPσ binding to GAG chains. This could prevent or decrease the ROCK pathway activation, finally leading to enhanced oligodendrocyte process outgrowth, axon myelination and regeneration at the injury site.

Binding between HB-GAM and heparan sulphate (HS) proteoglycans of the cell surface is also crucial for the success in HB-GAM induced neurite outgrowth effect. Glypican-2, an HS proteoglycan, has been identified as the most prominent cell surface component binding with HB-GAM. It has a glycosylphosphatidylinositol (GPI) linker by which it is attached to the cell membrane (Paveliev *et al.*, 2016). To support the finding, enzymatic cleavage of the GPI linkers of glypican-2 abolished the neurite outgrowth on CSPG substrate with added HB-GAM (Paveliev *et al.*, 2016). The general idea is that HB-GAM/CS complex binds to cell surface receptor glypican-2, which induces neurite regeneration (Paveliev *et al.*, 2016; Rauvala *et al.*,

2017). It is still unclear what is the exact mechanism of how the HB-GAM/CS complex driven ligation of glypican-2 leads to cell signalling, enhancing neurite regrowth. Glypican-2 does not have a cytosolic tail, so communication cannot be direct (Rauvala *et al.*, 2017). Suggested general mechanism is that HB-GAM links ECM GAGs to neuron surface GAGs provided by HSs of glypican-2.

Neurite outgrowth promoting effect of HB-GAM treatment has gained supportive evidence from both in vitro and in vivo studies. In vitro studies by Paveliev et al. (2016) showed that both instant coating and delayed addition of HB-GAM into primary CNS neurons plated on aggrecan had a promoting effect on neurite extension. HB-GAM was added to the culture medium at concentrations similar to those found in juvenile brain. The results lead to a conclusion that juvenile brain HB-GAM concentrations are required for reversing CSPG inhibitory effect on neurite outgrowth enhancement. Importantly, HB-GAM addition alone to the solution did not promote neurite outgrowth but displayed even some inhibitory effect, suggesting the importance of the binding with aggrecan or CS chains of other CSPGs in order to reach the neurite outgrowth inducing effect.

In addition, in vivo studies of the same research paper (Paveliev *et al.*, 2016) support these findings by showing that adult mice with spinal cord dorsolateral transection injury, treated with immediate HB-GAM injection (5 µl at 1 mg/ml) to the lesion site after the injury, caused a significant increase of the number of axons traversing the injured area from the caudal side, starting 14 days post-injury, continuing until day 28. Furthermore, HB-GAM treated axons had more branch points and varicosities compared to controls, which is consistent with the finding that axons with complex growth terminals are more likely to successfully regenerate across injury sites than axons with simpler growth terminals (Fenrich and Rose, 2011).

Since Paveliev et al. (2016) showed HB-GAMs positive effect on axonal regeneration, it is important to test whether the positive effect is also detectable at the functional level. Therefore, in this study, both the structural level via histological method detecting myelin of spinal cord grey matter and the functional level via the battery of behavioral tests were used. Two animal models, cervical hemisection and cervical hemicontusion were chosen since cervical SCI mouse models are very useful for modelling common cervical level SCIs in humans, both contusive and cut injuries. Since thoracic level mouse SCI models are tested more often than cervical ones, but the results are not directly translatable to cervical level injuries, it is crucial to further test and validate cervical level injury models, and to compare the differences of structural and functional recovery induced by the treatment between hemicontusion and hemisection models.

Overall, the clinical importance of SCI research is notable, since it is a globally significant and expensive condition, and with varying severity and extent of the symptoms between patients, and limited available treatment options, new treatment options are desperately needed for clinical use. The current study provides important insight considering the potential of HB-GAM treatment to enhance the recovery after SCI. Via the interaction between HB-GAM and CSPGs, the major inhibitory factors in the glial scar of injured spinal cord, HB-GAM can be seen as a promising treatment candidate.

2. Aim of the Study

The aim of the current study was to test and validate HB-GAM's therapeutic potential in posttraumatic functional recovery and structural regeneration using both cervical lateral hemisection and cervical lateral hemicontusion SCI models. A battery of behavioral tests was used to assess the functional outcome repeatedly over time, and histological methods to evaluate underlying anatomical alterations. In addition, using clinically relevant animal models enables further translation of experimental results to clinical-level research and use.

3. Materials and Methods

3.1 Animals

All experimental protocols for all animal experiments of the study were approved by ELLA-Animal Experiment Board in Finland (ESAVI/13202/04.10.07/2017). The methods for animal experiments were carried out in accordance with the guidelines of the Animal Experiment Board in Finland.

3R principles were followed in the study including the usage of as small as possible number of animals, still sufficient to provide results with appropriate statistical power, and taking into account the possible loss of animals due to surgery complications. Only the animals without obvious pain symptoms and normal body weight gain, able to active movements and normal feeding, were used in the post-surgery behavioral assessments. All surgeries were performed on the platform of Laboratory Animal Center.

50 adult female C57BL/6NHsd mice were obtained from commercial vendor at the age of 10 weeks and allowed to adapt for two weeks to the university facility with controlled room temperature (21 °C) and 12-hour light/dark cycle (lights on, 6:00 am). Mice were housed in individually ventilated cages in groups of 5 animals per cage provided with wooden bedding material, nestling material, and ad libitum food and water.

3.2 Experimental Design

After adaptation, the baseline behavioral tests were performed, including vertical grid, grip strength and open field test, in addition to baseline body weight measurements. Baseline

behavioral data were used to assign the animals to treatment groups. Experiment was started at the age of 12 weeks, and the experimental schedule is represented in Figure 1. Based on baseline behavioral tests and body weight, the mice were split into 2 models for hemisection and hemicontusion trauma: 5 cages containing all together 25 mice per trauma model. Seven mice were lost due to surgery or post-traumatic complications. After the surgery the remaining animals were assigned for vehicle control and HB-GAM treatment groups based on the trauma severity score and body weight measured on 7th day after trauma induction: 11 mice to the hemisection model with HB-GAM treatment, 10 mice to the hemisection model as vehicle controls, 11 mice to the hemicontusion model with HB-GAM treatment, and 11 mice to the hemicontusion model as vehicle controls. Intrathecal injections of HB-GAM or PBS were started on week one and continued once a week for four weeks. All experiments were performed in blinded method. Histological samples were taken on week 11.

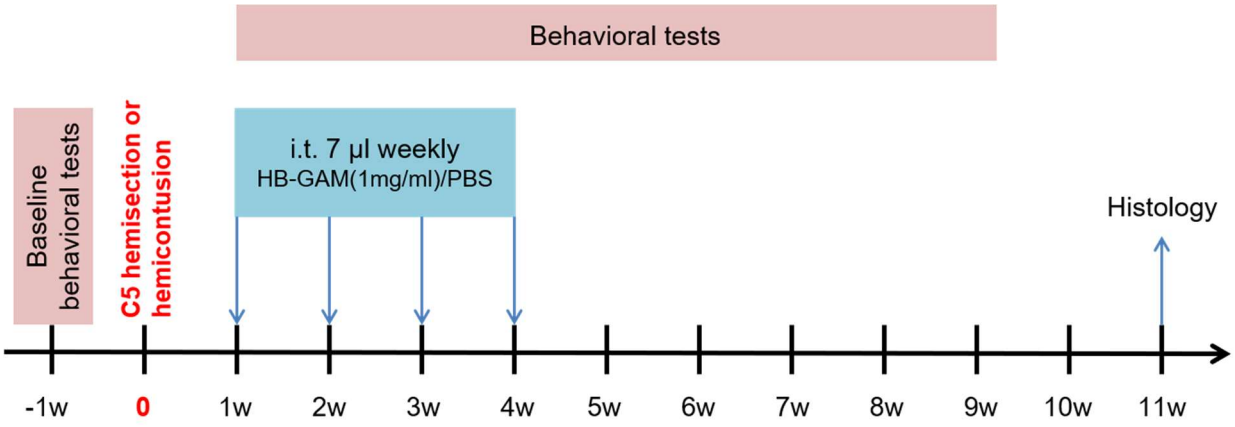

Figure 1. *Experimental schedule*. Baseline behavioral tests were performed one week before the spinal cord injury. One week after the injury, HB-GAM for test groups or PBS for vehicle control groups was delivered into the spinal canal in L5 area, and the injections were repeated once a week for four weeks. Behavioral assessments were performed starting from week one after the surgery until week 11. Mice were perfused and spinal cords were dissected during week 11, followed by microtome sectioning of the spinal cords and myelin gold chloride staining.

3.3 Pre- and Post-Surgery Care

Preoperational care for both trauma type group animals were similar; 15 minutes before surgery animals were injected with buprenorphine (Temgesic, i.p. 0.1 mg/kg) and enrofloxacin (Baytril, i.p. 5 mg/kg) to alleviate pain and to control bacterial infection. After the surgery, each animal was immediately injected with dexamethasone (Rapidexon, s.c. 0.2 mg/kg) to reduce inflammatory tissue swelling, 0.9% sodium chloride injection (s.c. 1 ml) to prevent dehydration, and postoperative pain was additionally alleviated with carprofen (Rimadil, s.c. 5 mg/kg). The mouse was then placed on a temperature-controlled plate set at 32.0 C until it regained the ability to move, and located back to home cage. Home cages were additionally provided with

wet food. Antibiotic and pain controlling treatment was continued for the following 3 days. Body weight and bladder emptying were checked daily during post-surgery days one to seven.

3.4 C5 Hemicontusion Model

Infinite Horizon Impactor was used for the hemicontusion injury. The procedure was adapted and modified from the work previously described (Plunet *et al.*, 2008). Animals were anaesthetized with isoflurane ventilation and placed to the heating pad (37°C) for surgery. Back area and the head area between ears were shaved, and the skin was disinfected with iodine solution (Betadine, 100 mg/ml). Dorsal midline skin incision over the lower cervical-upper thoracic part of spinal cord area was done. Then, dissection of the connective and muscle tissue was done in order to expose the posterior vertebral elements from C3 to C6, followed by C5 laminectomy to expose the spinal cord. T2 vertebra was used as a landmark for finding the C5 area. Spinal column was stabilized by holding below the C5 spine with a custom-built spinal stabilizer bars. After the laminectomy, the impactor tip (0.75 mm diameter with rounded edges made of carbon steel) was aimed at the right side of the grey matter of the dorsal spinal cord. Force of 75 kilodynes (kdyn) at 100 mm/s was delivered, followed by 15 seconds of continued compression. The actual impact force, tissue displacement, and velocity measured by the program were written down for each animal. After the contusion stabilizer bars were removed, the muscles were sutured with absorbable Monocryl suture and skin with non-absorbable Ethilon suture.

3.5 C5 Hemisection Model

Before the trauma exposure, the animals in the hemisection group received surgery procedure similar as the hemicontusion animals, including isoflurane anaesthesia, incision of skin and muscle, and exposure of C5 spinal cord. Laminectomy was followed by careful removal of the dura, and a 25G syringe needle was used for sectioning of the right cervical hemicord from midline dorsal vessel to the lateral side. Wound suturing, recovery, and post-surgery treatments were similar as the hemicontusion model.

3.6 Post-Surgery Recovery Assessment

Body weight gain and trauma severity were used as general health measurements for equally distributing animals to either HB-GAM treatment or vehicle control group. Body weight was measured before the surgery, daily during one week after surgery, and then weekly until the end of the experiment.

Trauma severity was subjectively evaluated at day 1 and day 7 after trauma by assessment of ipsilateral front paw grabbing ability. The mouse was held from its tail, hind paws detached from the metal grid of the home cage. Then, by slightly pulling the mouse from its tail, it was evaluated how the mouse used its front paws for grabbing the grid. Trauma severity was ranked

from 0 to 2, where 0 corresponds to no visible asymmetry in ipsilateral versus contralateral front paw grip, 0.5 to a very light trauma with slight weakness of ipsilateral paw grip and occasional paw misplacement, 1 to a moderate trauma with obvious ipsilateral paw grabbing problems abilities and paw misplacement, and 2 to a very severe trauma with no use of ipsilateral front paw for grabbing.

3.7 Experimental Treatment with Intrathecal Injections

Recombinant HB-GAM was produced as previously described (Raulo *et al.*, 1992). Intrathecal injections were done in order to deliver either 7 µl HB-GAM (1 mg/ml) for experimental groups or 7 µl 1 x PBS for vehicle control groups into the spinal canal's cerebrospinal fluid in the L5 spinal cord area. The injections were delivered 4 times, one injection per week, started from week 1 after the spinal cord trauma (Fig. 1). For injection the animals were anesthetised with isoflurane chamber, skin was shaved and disinfected with iodine solution (Betadine, 100 mg/ml) in the lumbar area. The L5 vertebra was localized between the iliac crests of the hip bones, and after the puncture of the skin by a 31G needle, a tail flick reflex was used as an indicator for puncturing the dura mater between the L5 and L6 spinous process, followed by slowly injecting the solution.

3.8 Behavioral Assessment

Vertical grid climbing, grip strength, open field, and von Frey tests were included in the behavioral test battery designed for evaluating the functional recovery after the trauma. The tests were performed repeatedly starting from the first week after surgery until 11 weeks after surgery (Fig. 1).

3.8.1 Vertical Grid

Vertical grid test was used to evaluate the climbing abilities and motor coordination recovery after trauma. Mice were placed individually to a horizontally positioned wire screen (25 x 22 cm, diameter of wires 2 mm spaced at 1cm), facing the edge. Immediately, the grid was turned to vertical position in a way that the mouse was positioned upside down at the lower edge. The time that the mouse spent turning to upward position and climbing up to the upper edge of the grid was measured. If the animal dropped, it was defined as a 60-second trial. If the animal did not reach the uppermost part of the grid within 60 seconds, trial was also defined as 60 seconds. The average of three trials of each week were used for statistical analysis.

3.8.2 Grip Strength

Grip strength test was used to measure the forelimb strength of both front paws and recovery after trauma, by an automated grip strength meter (Ugo Basil, Italy). Mice were allowed to grasp a mesh bar of the apparatus, while being held by the tail. When the mouse grasped the bar with its front paws, it was gently pulled away until it released the bar. The apparatus measured the

maximum strength of the grip. Measurement was repeated 5 times with at least a 1-minute interval. The average of every 5 trials was calculated and used for statistical analysis.

3.8.3 Cylinder Test

Cylinder test was used to evaluate the forelimb usage asymmetry after surgery and the functional recovery of the injured front paw. Mouse was put into a clear Plexiglas cylinder (13 cm diameter and 15 cm high), and a mirror was placed on the angle on the opposite side of the cylinder for better observation of the front paw use during the rearings. Use of ipsilateral (right) front paw, contralateral (left) front paw or simultaneous usage of both front paws were counted for the first 20 individual rearings with the cut-off time set at 5 minutes. If the mouse performed less than 5 rearings during the 5-minute session, it was excluded from the analysis. All sessions were videotaped to be able to check unclear situations.

3.8.4 Open Field

Open field test was used to measure locomotor activity and anxiety-like behavior of mice. Transparent plexiglass arena (30 × 30 × 20 cm, Med Associates, St. Albans, VT, illumination about 100 lx) equipped with infrared light sensors (at 1.5 cm intervals; 1.5 and 6 cm above the floor level) was used for automatic detection of horizontal and vertical activity. Each mouse was placed in the corner of the arena facing the corner and allowed to explore the arena for 15 min. Ambulatory distance, time spent in the center zone (anxiety parameter), and number of rearings were measured and analysed by the Activity Monitor v5.1 software (Med Associates, At. Albans, VT).

3.8.5 von Frey

von Frey test is a common method for measuring of pain sensitivity both in human patients and animals. Mice were placed on individual arenas with non-transparent walls and a grid floor and allowed to habituate for 30 minutes. Then, von Frey test apparatus with an attached mechanical von Frey filament was placed under the middle area of the palm of either left or right hind paw of the animal, and the filament was pushed toward the palm with increasing force, until the withdrawal of the paw. The measured latency (seconds) to the paw withdrawal was written down. Then, the other paw was tested. Measurement was repeated 4 times for each paw with at least 4-minute intertrial interval.

3.9 Perfusion and Spinal Cord Dissection

Each mouse was injected (i.p) with 0.25 ml Mebunat Vet (15 mg/ml) to reach deep anaesthesia that was validated by the absence of reaction to paw pinching. The heart was exposed, and the perfusion was performed. Each animal was perfused with 50 ml of PBS for 5 minutes, followed by 4 % PFA perfusion (100 ml per mouse, speed 19.6 rpm). Spinal cords were dissected from

spine and stored in falcon tubes containing 4 % PFA overnight at +4 °C, then in 30 % sucrose for 24 h at +4 °C or until the spinal cords were not floating anymore.

3.10 Freezing and Sectioning of the Spinal Cord Samples

About 1.5-2 cm long pieces of the spinal cords containing whole cervical area were frozen into the blocks with the Tissue Tek OCT on dry ice. The samples were stored at -80 °C.

Spinal cord samples were sectioned with a cryomicrotome (CM 3050 S, Leica) for 40 µm sagittal sections at -20 °C. Every fourth section was used for further histochemical analysis. The sections were stored in cryoprotection solution (1 l containing 300 g sucrose, 500 ml 1 x PBS, 10 g PVP 40, and 300 ml Ethylene-Glycol) at -20 °C.

3.11 Chemical Myelin Gold Chloride Staining and Image Analysis

Gold chloride staining for myelin was done as described in Laitinen et al. (2010).

The staining was done in two batches, separate days, with half of the spinal cord section samples in one batch, and the other half in one batch. The sections were mounted on microscope glasses, washed in 3 x 0.1 M PB (10 minutes, 28 minutes, 10 minutes), and dried overnight at +37 °C. Then the sections were incubated on a shaker (12 rpm) in a 0.2% gold chloride solution ($HAuCl_4 \cdot 3H_2O$, G-4022 Sigma-Aldrich) made in 0.02 M phosphate buffer (pH 7.4) containing 0.09% NaCl. The incubation time was 2 hours 49 minutes for the first batch, and 3 hours 36 minutes for the second batch, while the axon staining in the grey matter of the sections was checked with microscope every hour. The sections were then washed 3 x 10 minutes in 0.02 M phosphate buffer containing 0.09 % NaCl, followed by dehydration through an ascending series of ethanol (2 minutes in 50 % EtOH, 2 minutes in 70 % EtOH, 3 minutes in 96 % EtOH, and 2 x 3 minutes in absolute EtOH). Then, sections were cleared in xylene (3 x 5 minutes), followed by mounting with DePeX -mounting medium (#06522 Sigma-Aldrich, Lot # BCBV8243) and coverslipping.

Stained sections were scanned at the Institute for Molecular Medicine Finland (FIMM), using 3D HISTECH Pannoramic 250 Flash III, with 20x (NA 0.8) air objective. From the scanned images, one spinal cord section with the subjectively evaluated biggest trauma area per animal was selected for further analysis of myelin optical density measurements. All images were zoomed with 5x in CaseViewer version 2.2 or 2.3, followed by 8-bit edition in Fiji, with optical density calibration. Myelin optical density in the grey matter was measured approximately 100 to 200 µm from both rostral and caudal side of the trauma, using an oval area selection tool to select an area of a symmetric circle shape.

3.12 Statistics

Statistical analysis was done with SPSS Statistics 24 and GraphPad Prism 8 statistical packages. Data were tested for normality by Saphiro Wilk test, and the homogeneity of variance. Outlier data were defined as values exceeded +/-2SD from group mean value for every single time point and excluded from analysis. The treatment effect for normally distributed behavioral data with assumptions met for parametric statistical tests was analysed with repeated measures two-way ANOVA with Bonferroni post-hoc test (body weight, grip strength, and open field test parameter ambulatory distance), and independent samples t test (injury parameters displacement and velocity, and von Frey test). Myelin optical density data was normally distributed with assumptions met for parametric statistical tests, and were analysed with one-way ANOVA with staining day as covariance. Since there is no analog test available for repeated measures two-way ANOVA when data are not normally distributed, not normally distributed behavioral data (cylinder test, vertical grid test, and open field test parameters center zone time and rearings) were analysed with nonparametric Mann-Whitney test for every individual time point. Also, the injury parameter actual force was not normally distributed and was analysed with nonparametric Mann-Whitney test. Statistical significance was set at $p<0.05$. All data are presented as the mean +/- the standard error of the mean (SEM).

4. Results

4.1 Recovery and Injury Parameters

Injury parameters of the hemicontusion model included actual force, displacement and velocity (Table 1). There were no statistically significant differences between the HB-GAM treated and control animals in any of the injury parameters, so it can be concluded that the trauma was equal enough to all animals in the contusion model.

Injured animals in both models had problems with the contralateral front paw usage after the injury (Fig. 2A hemicontusion; Fig. 3A hemisection).

The body weight before injury did not significantly differ between the HB-GAM treated and control animals in either hemicontusion or hemisection model. All animals had a drop of the body weight after the surgery. The body weight was gained after the post-surgery drop from week 4 to 10 (Fig. 2B hemicontusion; 3B hemisection), in both HB-GAM treated and control mice of both injury models.

Table 1. Injury parameters of the hemicontusion trauma model. Actual force, Displacement and Velocity, mean and standard error of the mean (SEM) values of vehicle control and HB-GAM treated individuals.

Trauma	Treatment		Actual force (kdyn)	Displacement (μm)	Velocity (mm/s)
Hemicontusion	Control	**Mean**	81.0	1070.2	121.0
		SEM	1.8	89.3	1.0
Hemicontusion	HB-GAM	**Mean**	84.9	895.2	122.2
		SEM	2.5	92.6	0.9

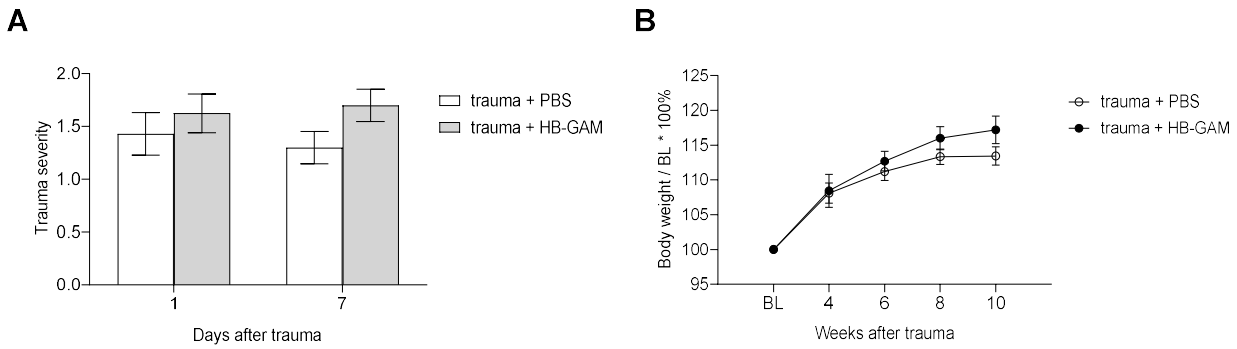

Figure 2. *Post-surgery recovery assessment of mouse cervical hemicontusion model.* (**A**) Trauma severity of the ipsilateral front paw on the next day and 7 days after trauma induction. (**B**) Body weight gain normalised to baseline (BL) measurements.

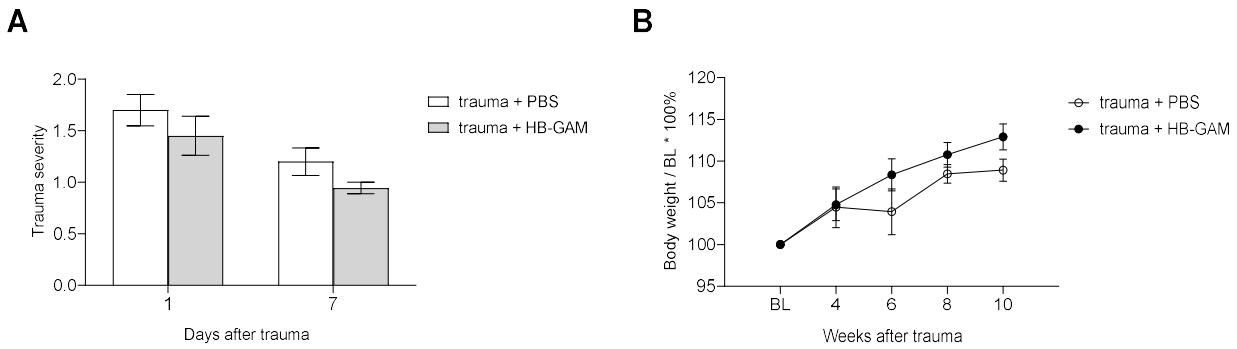

Figure 3. *Post-surgery recovery assessment of mouse cervical hemisection model.* (**A**) Trauma severity of the ipsilateral front paw on the next day and 7 days after trauma induction. (**B**) Body weight gain normalised to baseline (BL) measurements.

4.2 Functional Assessment in the Mouse Model of Cervical Spinal Cord Hemicontusion

4.2.1 Vertical Grid

There were no significant differences between the HB-GAM treated and vehicle control mice in the vertical grid test. Both showed increased time required for climbing during week 2 after surgery, with relatively stable and moderate improvement until week 8, followed by an increase of climbing time from week 8 to 11 (Fig. 4A).

4.2.2 Grip Strength

Both groups showed a decrease of grip strength after the surgery. Statistical analysis did not reveal significant differences between HB-GAM treated and vehicle control mice in grip strength over the following 8 weeks after the trauma exposure (Fig. 4B).

4.2.3 Cylinder test

Both HB-GAM treated and vehicle control mice were very inactive during the first post-surgery week, with no significant improvement during the following weeks, and no statistically significant differences between the groups (Fig. 4C).

4.2.4 Open Field

The ambulatory distance was diminished during the first post-surgery week in both groups, with no statistically significant difference between HB-GAM treated and vehicle control animals (Fig. 4D). The parameter measuring anxiety-like behavior, time spent in the center zone of the maze, had no significant differences between the HB-GAM and vehicle control mice. In both groups, there was a decrease of center zone time after the trauma on post-surgery week 1, with no significant improvement, indicating increased anxiety-like behavior (Fig. 4E).

4.2.5 von Frey

There was no asymmetry detected in left and right hind paw reactivity in either HB-GAM treated or control group (Fig. 4F).

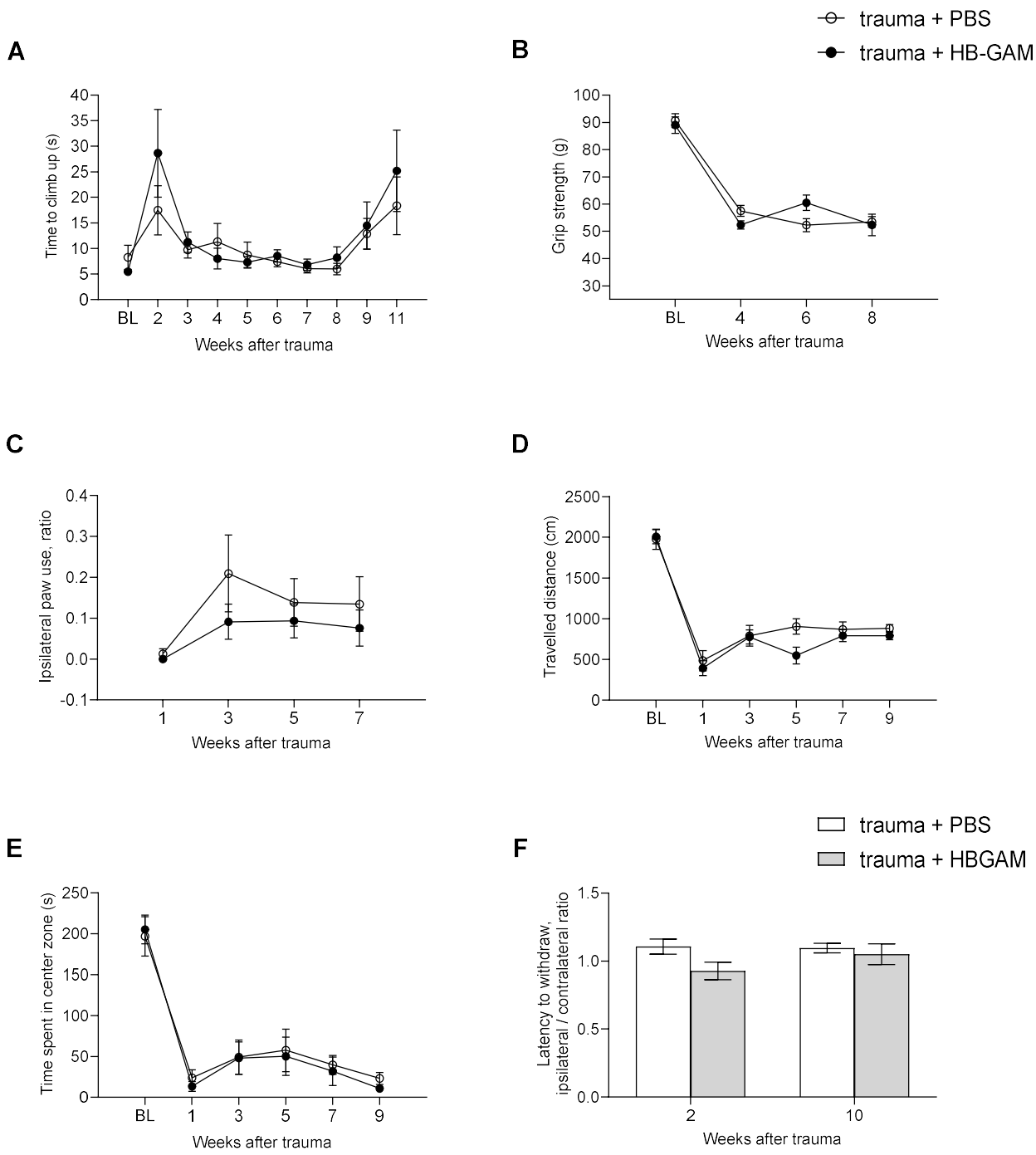

Figure 4. *Functional outcome of intrathecal HB-GAM treatment in mouse cervical hemicontusion model.* (**A**) *Vertical grid.* The latency to climb up to the top of the vertical grid. (**B**) *Grip strength.* Forelimb strength of both front paws. (**C**) *Cylinder test.* Ratio of ipsilateral front paw use. (**D**) *Open field.* Ambulatory distance travelled for 15 min in open field maze. (**E**) *Open field.* Time spent in center zone. **(F**) *von Frey.* Ipsilateral/contralateral hind paw ratio of the latency to withdrawal. Data represented as the mean value. Error bars indicate SEM, standard error of the mean.

4.3 Repeated i.t. Administration of HB-GAM Resulted in Some Enhancement of the Functional Recovery in Mouse Model of Cervical Spinal Cord Hemisection

4.3.1 Vertical Grid

HB-GAM treated mice improved their climbing abilities in a shorter time compared to vehicle control mice. In addition, HB-GAM treated mice almost completely recovered their climbing speed and spent significantly less time to reach the top of the vertical grid compared to vehicle control animals on week 3 after spinal cord trauma induction ($p=0.0233$ Mann-Whitney test; n=10 vehicle control; n=9 HB-GAM), while the vehicle control group reached its best performance only by week 6. Prolonged recovery of both groups lasted until week 6, but was surprisingly followed by repeated progressive increase of climbing time. Importantly, the repeated impairment of climbing performance was more prominent in vehicle control group than HB-GAM treated group, reaching the significant difference on week 11 ($p=0.0382$, Mann-Whitney test; n=10 vehicle control; n=10 HB-GAM) (Fig. 5A). There was also a trend of better performance of the HB-GAM treated animals compared to vehicle controls during week 9 ($p=0.0531$, Mann-Whitney test; n=9 vehicle control; n=9 HB-GAM).

4.3.2 Grip Strength

There was no significant difference in grip strength between the HB-GAM treated and control mice. Both treatment groups had decreased front paw grip strength after the injury compared to baseline level (Fig. 5B).

4.3.3 Cylinder Test

One week after the injury, animals in both HB-GAM and control groups showed nearly complete loss of ipsilateral, injured front paw use, calculated as a right/left paw number of rearings ratio (Fig. 5C). In general, the animals were very inactive during post-surgery week 1, and their activity increased during the later weeks. There was no statistically significant difference between the HB-GAM treated and control mice in the use of injured right front paw.

4.3.4 Open Field

The travelled distance in the open field maze did not differ between the control and HB-GAM treated mice (Fig. 5D). For both the HB-GAM treated and control mice, the ambulatory distance decreased after the trauma, being at the lowest level during week 1, with no significant improvement during the following weeks. The travelled distance did not differ between the HB-GAM and vehicle control groups. There was no significant difference in the time spent in the center zone between the controls and HB-GAM treated animals. After the surgery, the time spent in the center zone of the arena decreased for all traumatic animals compared to baseline and did not show improvements during the following weeks (Fig. 5E).

4.3.5 von Frey

There was no asymmetry detected in left and right hind paw reactivity in either the HB-GAM treated or control group (Fig. 5F).

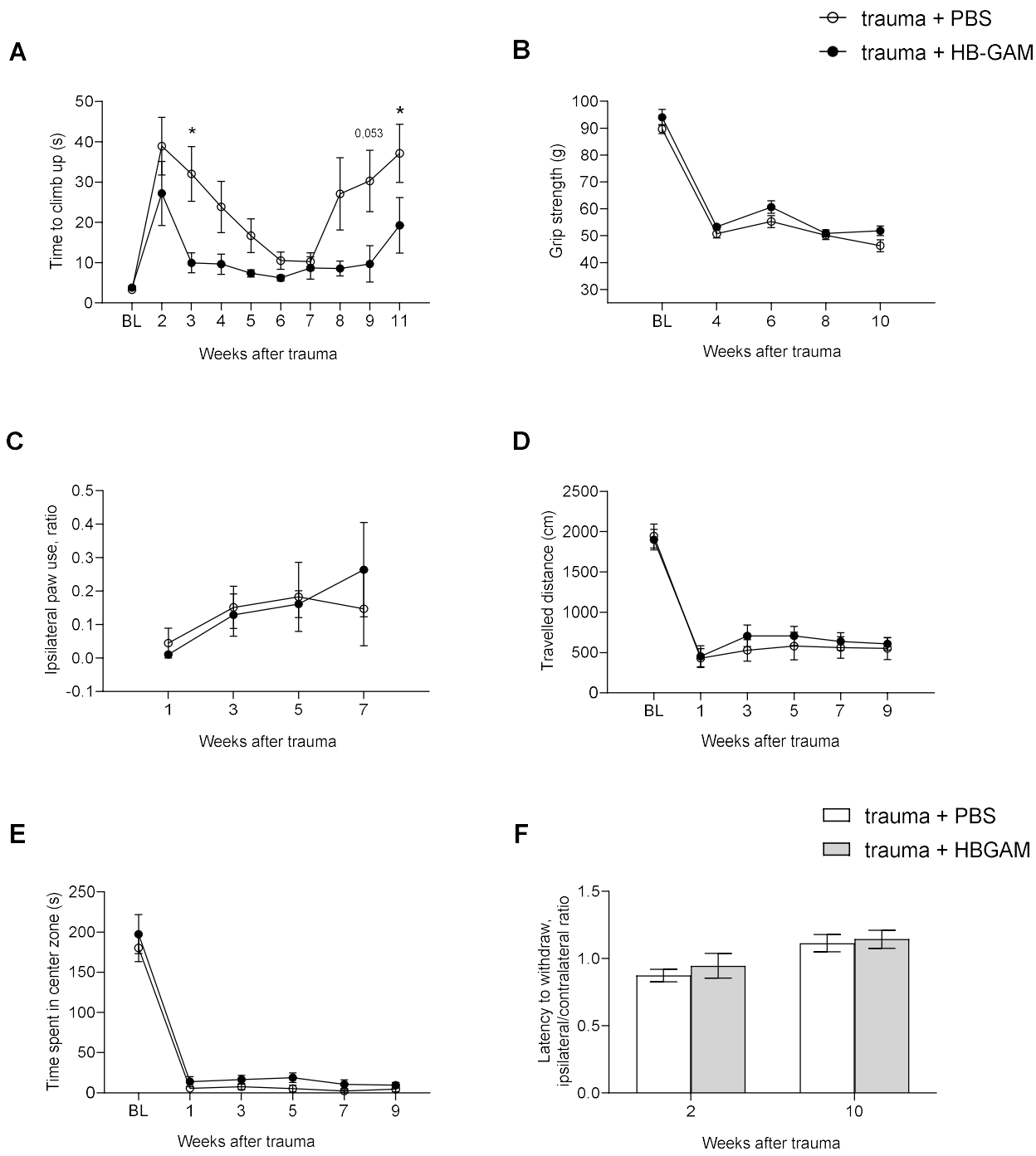

Figure 5. *Functional outcome of intrathecal HB-GAM treatment in mouse cervical hemisection model.* (**A**) *Vertical grid.* HB-GAM treated mice used less time to climb up to vertical grid in comparison with vehicle control mice. (**B**) *Grip strength.* Forelimb strength of both front paws. (**C**) *Cylinder test.* Ratio of ipsilateral front paw use. (**D**) *Open field.* Ambulatory distance travelled for 15 min in open field maze. (**E**) *Open field.* Time spent in center zone. (**F**) *von Frey.* Ipsilateral/contralateral hind paw ratio of the latency to withdrawal. *p<0.05, Mann-Whitney test. Data represented as the mean value. Error bars indicate SEM, standard error of the mean.

4.4 Repeated i.t. Treatment with HB-GAM Increased the Myelin Optical Density in Cervical Hemicontusion Injury Model, but Had No Effect on the Myelination in Cervical Hemisection Model

HB-GAM treated hemicontusion mice had higher grey matter myelin optical density in the rostral side ($p=0.0275$, one-way ANOVA with staining day used as a covariance; n=7 vehicle control; n=9 HB-GAM), and a trend of a higher optical density in the caudal side ($p=0.058$, one-way ANOVA, information of staining day used as a covariance; n=8 vehicle control; n=8 HB-GAM) of the trauma compared to vehicle control mice (Fig. 6A; Fig. 5).

Between the HB-GAM and vehicle control mice, there was no significant difference in optical density of the grey matter myelin on either rostral or caudal side of the trauma (Fig. 7A) in the hemisection model.

The example images of myelin-stained sections of both the HB-GAM treated and vehicle control mice are represented in figures 6B (hemicontusion, HB-GAM), 6C (hemicontusion, vehicle control), 7B (hemisection, HB-GAM), and 7C (hemisection, vehicle control), with magnified images of both rostral and caudal sides.

A

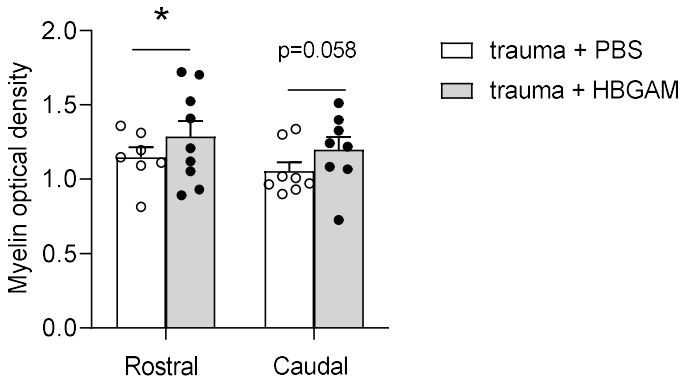
*
p=0.058
trauma + PBS
trauma + HBGAM
Myelin optical density
2.0
1.5
1.0
0.5
0.0
Rostral
Caudal

B

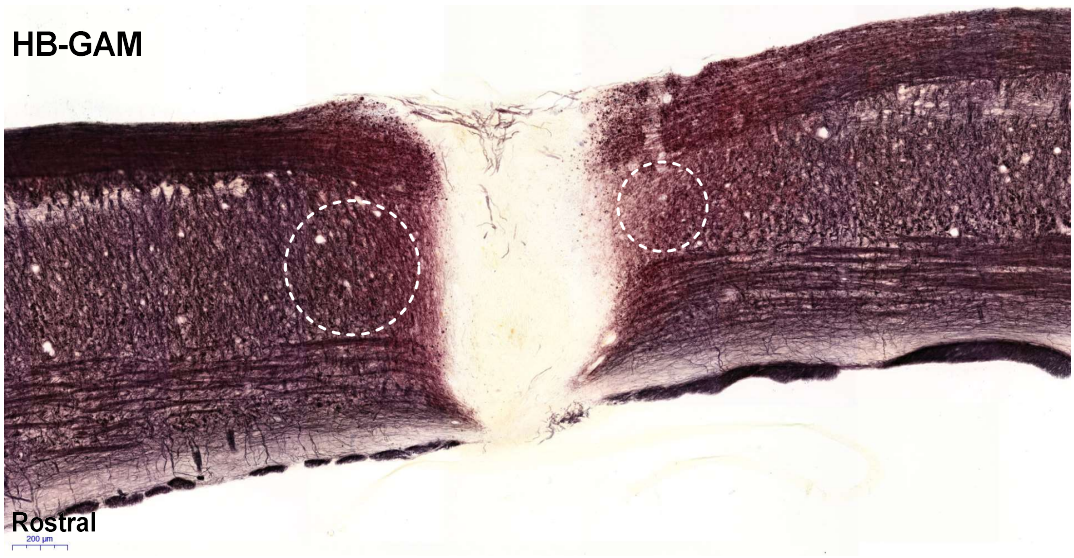
HB-GAM
Rostral

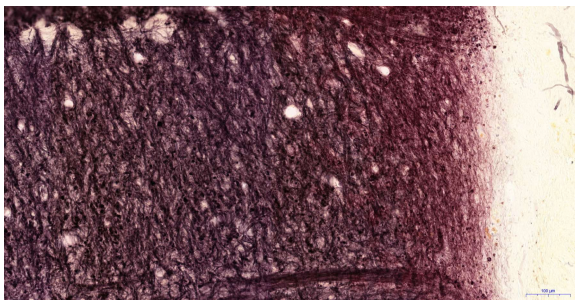

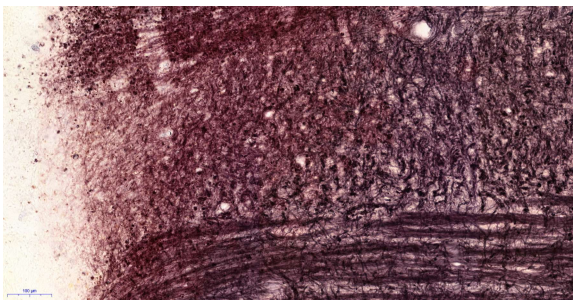

C

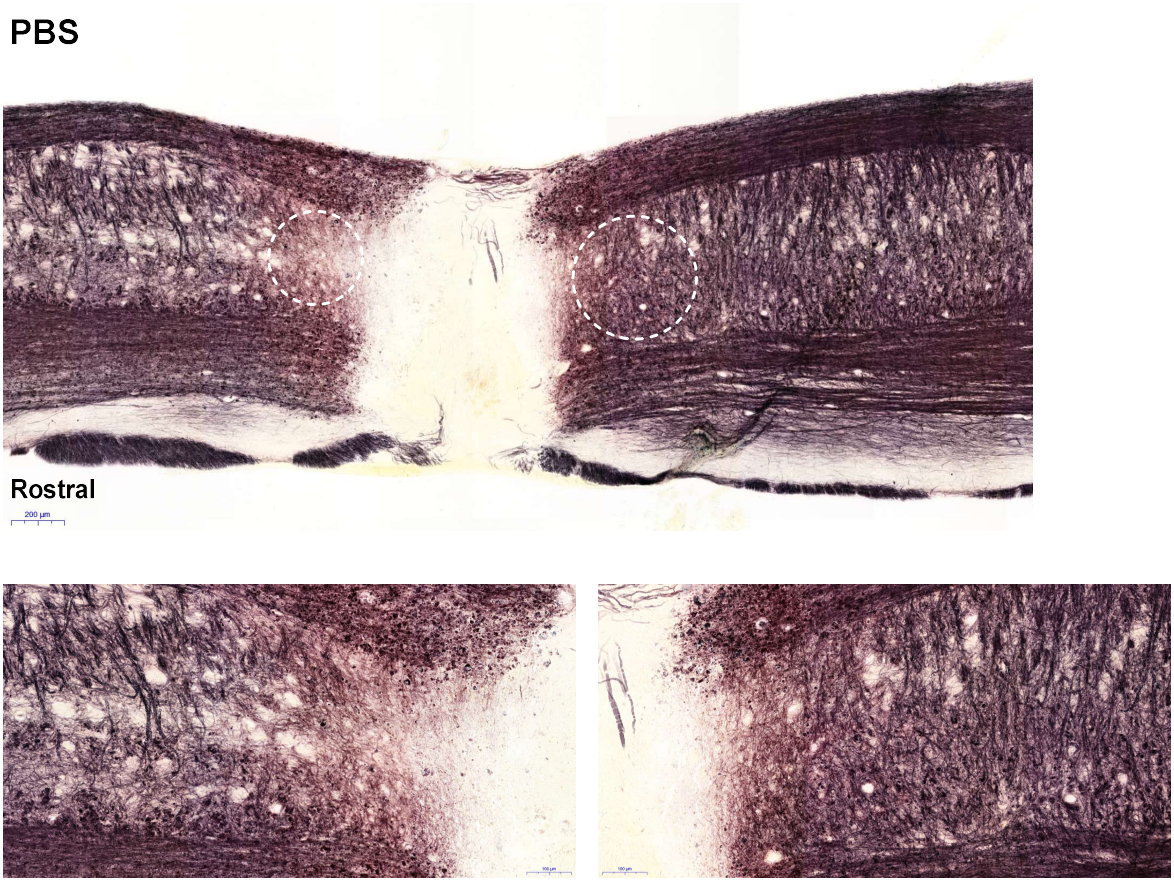

Figure 6. *Structural outcome of intrathecally injected HB-GAM treatment in mouse cervical hemicontusion model.* **(A)** Myelin optical density in grey matter on caudal and rostral side of the trauma was significantly higher in HB-GAM treated animals compared to controls. **(B)** Spinal cord sections of HB-GAM treated and **(C)** vehicle control mice. Magnification of the images is x5. The dotted circles approximately represent the areas of the grey matter that were used for analysis, and the images with bigger magnification are x15. *p<0.05, one-way ANOVA, information of staining day used as covariance. Scale bars in the x5 image are 200µm and in x15 100µm. Error bars indicate SEM, standard error of the mean.

A

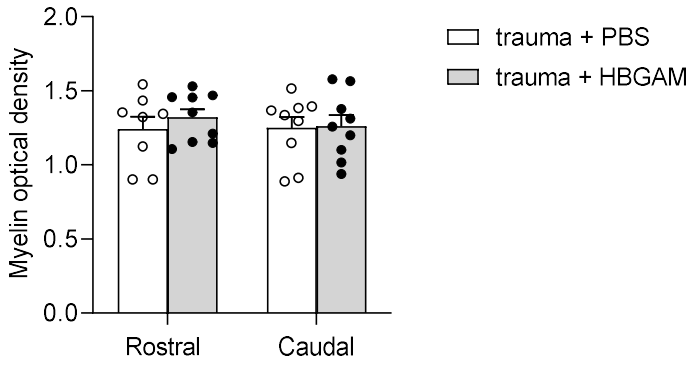
2.0
1.5
1.0
0.5
0.0
Myelin optical density
Rostral
Caudal
trauma + PBS
trauma + HBGAM

B

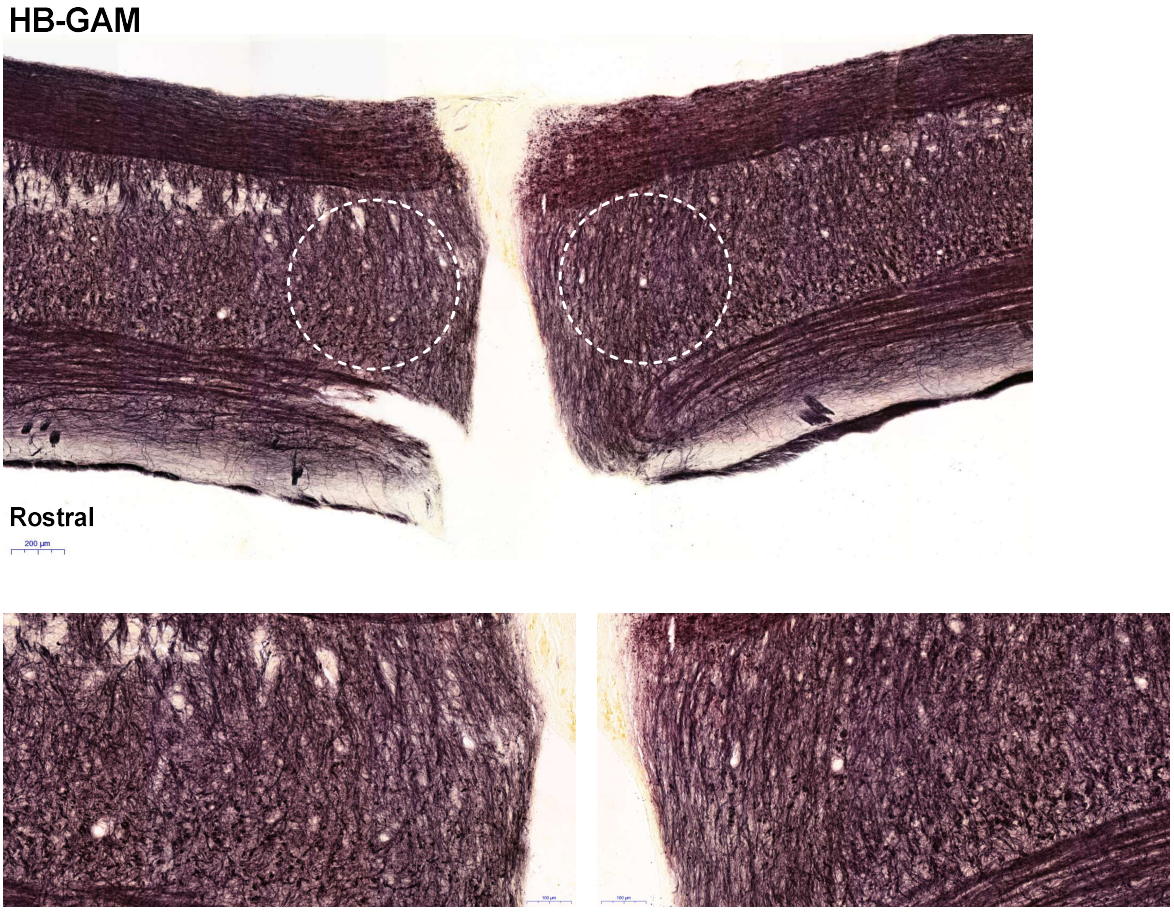
HB-GAM
Rostral

C

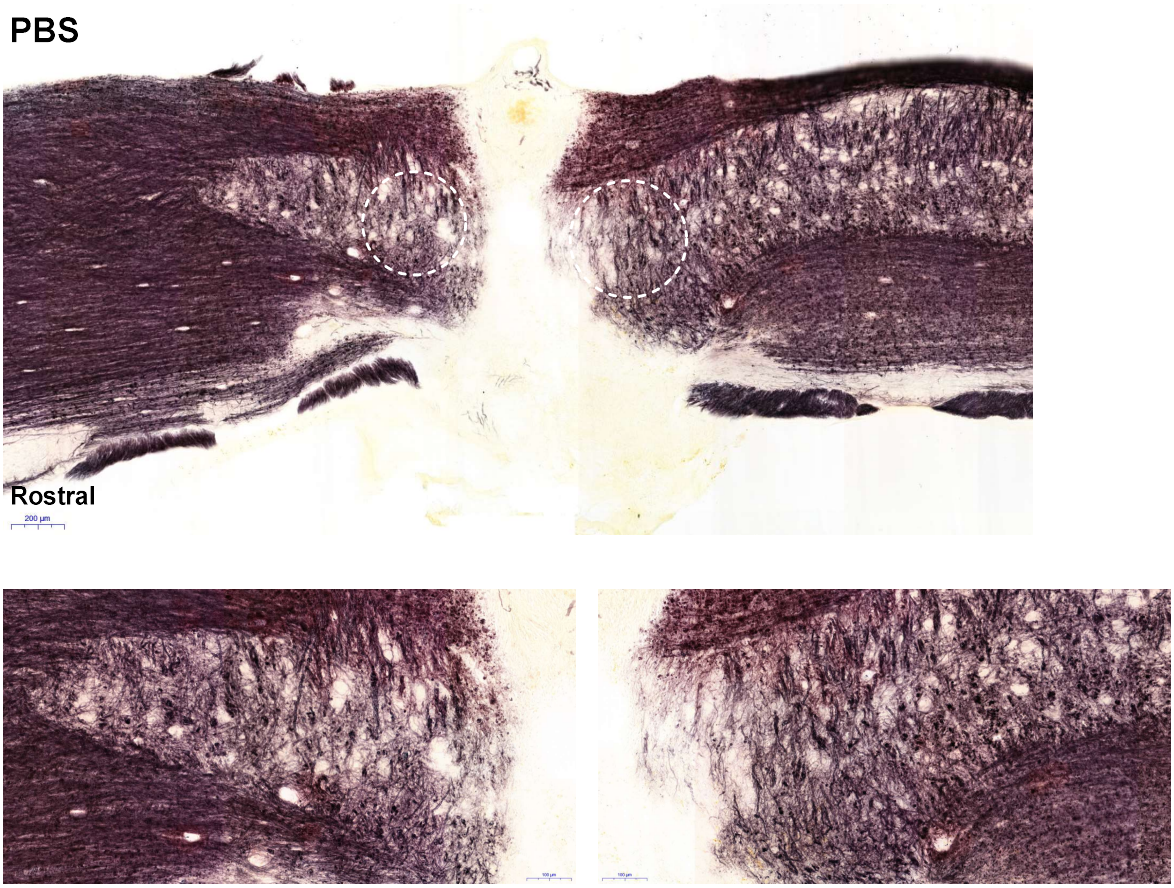

Figure 7. *Structural outcome of intrathecally injected HB-GAM treatment in mouse cervical hemisection model.* **(A)** Myelin optical density in grey matter on the caudal and rostral side from the trauma after hemisection injury did not differ between HB-GAM treated and control animals. $p>0.05$, one-way ANOVA, information of staining day used as covariance. **(B)** Spinal cord sections of HB-GAM treated and **(C)** vehicle control mice. Magnification of the images is x5. The dotted circles approximately represent the areas of the grey matter that were used for analysis, and the images with bigger magnification are x15. Scale bars in the x5 images are 200µm and in x15 100µm. Error bars indicate SEM, standard error of the mean.

5. Discussion

5.1 Main Findings

This study showed that HB-GAM had an improving effect on functional recovery in hemisection trauma model in vertical grid test. Importantly, the improved climbing performance was not associated with elevated front paw muscle strength or locomotor activity of the HB-GAM treated animals, or altered anxiety-like behavior or hind paw tactile sensitivity, since the tests measuring these parameters showed no treatment effect. However, since the positive treatment effect was not visible in other behavioral tests than vertical grid, there is a need for further studies to explore whether HB-GAM could induce functional recovery in a wider range, and which behavioral tests are suitable for detecting the effect. Furthermore, hemicontusion trauma model showed no functional recovery induced by HB-GAM treatment, and hence there is a need for

further testing and validating the exact differences in functional recovery between the SCI trauma models.

The results of structural recovery showed that the measured optical density of grey matter myelin was significantly higher in the HB-GAM treated hemicontusion model compared to the vehicle control group, but no difference was found between the hemisection model treatment groups.

Since the two trauma models have fundamentally different features, it is logical that they also showed different responses in both functional and structural recovery. For example, as mentioned earlier in the text, hemisection model allows a very precise trauma area to be selected, with the more precise detection of the regeneration of injured axons (Sharif-Alhoseini *et al.*, 2017), whereas the severity and expansion of the hemicontusion injury is more difficult to control, and to evaluate the actual regeneration of axons. In addition, the inflammatory attack is more severe in hemicontusion model, and it also may in part have an effect on the different responses in the functional and structural recovery. However, the exact mechanisms between these features and functional and structural responses of the SCI models are very complicated, and hence hard to prove.

It can be expected that the increased myelin optical density in the area of the injury could be beneficial for functional recovery, since an injury to the cervical area often causes disruption of nerve tracts crucial for ipsilateral front paw functioning. However, since the hemicontusion model displayed only structural recovery, and the hemisection model showed only functional recovery, it is crucial to continue to study whether there is a connection between functional recovery and myelin optical density specifically in different SCI models.

5.2 Comparison to Related Studies

This study provides partial support to the earlier findings of HB-GAM being an enhancing factor for neurite outgrowth and structural recovery in vitro and in vivo (Paveliev et al., 2016), and a slight evidence for its probable importance in the functional recovery after cervical SCI in mice, which is not yet widely studied.

The results showed increased myelinization in grey matter in the HB-GAM treated hemicontusion model, but not in the HB-GAM treated hemisection model. As described in the introduction, CSPGs, with PTPσ and its downstream ROCK-pathway, are key factors inhibiting myelination after CNS injuries (Pendleton *et al.*, 2013). While ChABC treatment has been shown to reverse the inhibitory effect of CSPGs (Pendleton *et al.*, 2013), this study provides evidence that HB-GAM treatment could be beneficial for reversing CSPG-driven myelination inhibition after SCI injury, probably via the competition between HB-GAM and PTPσ binding to CS side chains of CSPGs, and further affecting the downstream ROCK pathway and

myelination, at least in the cervical hemicontusion model. However, in addition to its neurite outgrowth promoting effect via interaction with CSPGs, HB-GAM has been shown to moderately improve oligodendrocyte differentiation on aggrecan-coated substrates, probably due to the same interaction mechanism with CSPGs as with neurons (Kuboyama *et al.*, 2017). Therefore, it is reasonable to widen the research of HB-GAM in order to take into account its probable potential effect on other factors of the glial scar, and also other spinal cord lesion structures and cellular level factors, including oligodendrocytes and myelination.

5.3 New Study Problems and Possible Applications of the Study

There is a need for evaluating safe but proper doses and timing for HB-GAM treatment. It has already been shown that in mice, high doses (up to 10 mg/ml) in adults showed no toxicity (Paveliev *et al.*, 2016), and overexpression of HB-GAM in transgenic mice did not show any noticeable health problems, brain histology changes or behavioral problems (Pavlov *et al.*, 2002). Instead, there was enhanced learning in water maze and decreased anxiety-like behavior in elevated plus-maze compared to HB-GAM knockout mice with an opposite behavioral phenotype (Pavlov *et al.*, 2002). This study included HB-GAM treatment of sub-chronic trauma, but the applications for the treatment of chronic trauma are needed as well. With the chronic trauma models, there should be additional CNS stimulation combined with the treatment in order to guide the neurite outgrowth. The chronic model would be very significant since most of the patients have chronic SCI symptoms, lasting for years.

One possible target for HB-GAM treatment could be multiple sclerosis (MS), a disease with chronic demyelination. Due to chronic inflammation in the CNS with still poorly understood detailed mechanisms, myelin membranes and oligodendrocytes are destroyed (Chamberlain *et al.*, 2016). The CSPGs aggrecan, neurocan, and NG2 inhibit oligodendrocyte process outgrowth and myelination of injured axons (Pendleton *et al.*, 2013), and are also upregulated in the ECM within active demyelinating lesions of MS (Sobel and Ahmed, 2001). In addition, CSPGs bind to oligodendrocyte progenitor cells (OPCs) via PTPσ, which is known to result in inhibition of the remyelination process in MS (Luo *et al.*, 2018). Hence it would be interesting to test whether HB-GAM treatment could be beneficial for MS patients by increasing the myelination via reversing the inhibitory effect of CSPGs.

5.4 Research Ethics

Ethical matters were carefully considered in this study. Since the surgeries are very invasive, and have risks for complications and inflammation, animals were treated with analgesic and anti-inflammatory drugs both pre- and post-surgery. In addition, sodium chloride was injected after surgery in order to avoid dehydration. 3R principles were followed by precise and careful experimental design, where the number of animals was kept as low as possible, but also

considering the possible loss of individuals during the experiment, and still being able to provide statistically significant results. Group-housing was selected in order to avoid emotional problems common in single-housed mice.

5.5 Critical Evaluation of the Study

In general, animal models are very useful for SCI research, but the disadvantage is that the results are not directly translatable to clinical use. Mouse as a model animal has its limitations since it is not directly comparable to humans due to the differences in the size of the body, metabolic properties, and quadrupedal versus bipedal movements. Furthermore, it is also crucial to test the effectiveness of HB-GAM treatment in other animal species, for example swine and primates, in order to reach more human-like features, enabling more comparable environment of the injured spinal cord, and more reliable testing of suitable doses and timing of the treatment.

When performing behavioral tests, there are multiple factors and parameters that need to be carefully evaluated in order to provide reliable and replicable research. During behavioral tests, any bias was avoided by performing the repeated trials of the tests as similarly as possible. The handling of animals was calm, and loud voices were avoided. However, when the behavioral tests are performed in a unit with multiple other users, there is always a risk for alteration in background voices and surprising interruptions, that might have an effect on animals' stress levels, possibly affecting the results in an unexpected way. In addition, it is important to point out that each animal has individual variability in behavioral properties and stress sensitivity, all effecting on the results in some way.

In vertical grid test, there was a notable improvement of the climbing performance in the HB-GAM treated group of hemisection model, and the recovery of climbing abilities almost reached the baseline level (Fig. 5A). However, the climbing time started to increase after the notable improvement in both vehicle control and HB-GAM groups. The similar increase of climbing time was also seen in the hemicontusion group (Fig. 4A), so the worsened climbing performance was not trauma-specific. Even though there was elevated post-surgery anxiety-like behavior detected in both HB-GAM treated and vehicle control groups of both trauma models, it cannot fully explain the increased climbing time since the time spent in center zone remained at similar levels during all post-surgery weeks. In addition, there was not alterations of hind paw tactile sensitivity or allodynia measured by von Frey test, or bodyweight, so one of the possible reasons for the increased climbing time could be motivational. It would be interesting to combine HB-GAM treatment with enriched environment that has been shown to help to prevent motivation decline and provide general stimulating effect to neuronal plasticity (Le Bras, 2019).

Cylinder test is an effective way to evaluate the usage of front paw for postural support and vertical exploration and the recovery of the injured paw motor and sensory functions after the trauma. Baseline assessment of the cylinder test was not included in this study, but earlier findings have shown that typically, there is quite equal use of both front paws for rearings, with ~20% only either left or right front paw, and ~60% both front paws simultaneously (Streijger *et al.*, 2013). Typically, the contralateral forelimb usage during rearings is dramatically reduced after injury, which is thought to be related to the disruption of axons and the eradication of motor neurons at the lesion epicenter, which innervates multiple muscles participating in forelimb movements (Soblosky, Song and Dinh, 2001).

Open field test ambulatory distance is a widely used parameter for examining locomotor activity in experimental animals. Thigmotaxis means the tendency to remain close to walls of the open field arena, and the software calculates the time spent in inner versus outer zones, presenting them as a function of total time in the arena (Seibenhener and Wooten, 2015). This study showed no difference in the ambulatory distance or the measured time spent in the center zone between vehicle controls and HB-GAM treated mice in either model, so it is possible to conclude that treatment did not alter locomotor activity and had no anxiogenic effect. Overall, the results indicate that either differences in locomotor activity or anxiety-like behavior could not explain the observed results of other functional tests.

von Frey test is used for testing and excluding whether the injury or treatment has led to development of any unwanted plasticity with allodynia, when non-painful stimuli become painful (Deuis, Dvorakova and Vetter, 2017). In general, it is known that allodynia is a possible side effect of central spinal plasticity (Treede and Magerl, 2000). In addition, lesion can further involve neuropathic pain (Gwak *et al.*, 2012), which may be attenuated or exaggerated by treatment, and changes in sensory functions can have an impact on locomotor functioning. During the von Frey test, animals' hind paws are exposed to a nociceptive stimulus, a von Frey filament, with increasing pressure. If the subject withdraws from the stimulus that normally does not evoke a withdrawal, it can be considered to have allodynia. Paw withdrawal threshold is defined as the minimum force eliciting a pain response (Detloff *et al.*, 2012). In this study, allodynia was excluded since there were no statistically significant difference in the withdrawal latency between ipsilateral and contralateral hind paw in either vehicle control or HB-GAM treated mice in either trauma model.

In this study, the freezing and sectioning of the samples were done as accurately as possible since there is always a risk for the sample not to be completely straight in the freezing mold and in the holder of the microtome. Histological staining was also done as carefully as possible, following the instructions of the used protocol.

Chemical myelin gold chloride method was chosen for this study since it provides a sensitive and high-resolution marker for CNS myelin that reaches individual myelinated fibers and allows quantitative analysis of regeneration in myelin structures surrounding axons. Savaskan et al. (2009) showed that gold particles stain CNS outer, compact, and inner axon layers in a similar manner, independently of the axonal diameter (120 to 260 nm). In addition, gold particles were shown to stain myelin protein components of brain sections, but shiverer/MBP-deficient mice had similar staining intensity as control mice, indicating that stained protein structures do not include myelin basic protein (MBP) but other protein components. There are also other available methods for myelin staining, including myelin antibody-based immunocytochemistry staining of myelin specific proteins, a staining method based on the detection of the specific lipid composition of myelin, and silver staining techniques (see in Savaskan *et al.*, 2009). However, those techniques have several disadvantages and most of them do not reach the single fiber resolution required for this study, so the chemical myelin god chloride method was considered as the most suitable approach.

5.6 Concluding Remarks

The current study provided valuable results showing that the two cervical level SCI models have different responses in both functional level recovery and structural regeneration induced by HB-GAM treatment. The cervical hemicontusion model showed structural regeneration measured by spinal cord grey area myelin optical density, whereas the cervical hemisection model showed functional recovery only in the vertical grid test of the battery of behavioral tests. The different features of the trauma models partly explain the different ways of recovery, and importantly, the results highlight the need to test and validate each treatment candidate's effect on each trauma model. In addition, the trauma type specific relationship between functional and structural recovery must be studied in more detail.

There is a need for further study of the mechanisms of cellular and tissue level of SCI. While the complicated structure and interactions of multiple cell types and factors of glial scar will be understood better, it eventually potentiates the finding of new treatment targets and candidates. Considering especially this study, the actual mechanisms of HB-GAM's positive effect after SCI are very important to study more comprehensively, including also other interactions in addition to those shown between HB-GAM and CSPGs. Furthermore, HB-GAM treatment will probably be useful for multiple types of CNS injuries and degenerative CNS diseases.

To conclude, the current study provided some promising evidence of HB-GAM as a potential treatment candidate for SCI, inducing structural regeneration in the cervical hemicontusion model, and a slight functional recovery in the cervical hemisection model. Furthermore, by understanding the mechanisms and recovery-associated systems of SCI more

comprehensively, the research will hopefully provide more treatment options and combinations for SCI patients, with more targeted and individual possibilities for clinical use.

6. Acknowledgements

I would like to thank my supervisors Heikki Rauvala and Natalia Kulesskaya for their support and advice during the project, and also for the opportunity to be part of the research group as a graduate student. Furthermore, a special thank you to Natalia Kulesskaya for familiarizing me with behavioral work with mice, and also with the histological and statistical analyses. Next, I would like to thank Sami Piirainen for the advice and help especially with histological methods and statistics. Also, a grateful thank you to FIMM Digital Microscopy and Molecular Pathology Unit for the scanning of the spinal cord samples. In addition, I would like to thank Seija Lågas and Erja Huttu for their help with the laboratory work, and Anni Näsi for helping me with the final layouts of the graphics of this work. Finally, I would like to thank my family and friends for their support during the project.

7. References

Aguilar, R. M. and Steward, O. (2009) 'A bilateral cervical contusion injury model in mice: Assessment of gripping strength as a measure of forelimb motor function', *Experimental Neurology*, 221, pp. 38–53. doi: 10.1016/j.expneurol.2009.09.028.

Anderson, K. D. (2004) 'Targeting recovery: Priorities of the spinal cord-injured population', *Journal of Neurotrauma*, pp. 1371–1383. doi: 10.1089/neu.2004.21.1371.

Anderson, K. D., Abdul, M. and Steward, O. (2004) 'Quantitative assessment of deficits and recovery of forelimb motor function after cervical spinal cord injury in mice', *Experimental Neurology*, 190(1), pp. 184–191. doi: 10.1016/j.expneurol.2004.06.029.

Baumann, N. and Pham-Dinh, D. (2001) 'Biology of oligodendrocyte and myelin in the mammalian central nervous system', *Physiological Reviews*. American Physiological Society, pp. 871–927. doi: 10.1152/physrev.2001.81.2.871.

Berkowitz, M. *et al.* (1998) '"Spinal Cord Injury: An Analysis of Medical and Social Costs," Monroe Berkowitz, Paul K. O'Leary, Douglas L. Kruse and Carol Harvey, eds.', 32(1), pp. 3–3. doi: 10.1080/003655000750045659.

Bianchi, M. E. (2007) 'DAMPs, PAMPs and alarmins: all we need to know about danger', *Journal of Leukocyte Biology*, 81(1), pp. 1–5. doi: 10.1189/jlb.0306164.

Bradbury, E. J. *et al.* (2002) 'Chondroitinase ABC promotes functional recovery after spinal cord injury', *Nature*, 416(6881), pp. 636–640. doi: 10.1038/416636a.

Le Bras, A. (2019) 'Environmental enrichment increases neuroplasticity and recovery after SCI', *Lab Animal*. Nature Publishing Group, p. 163. doi: 10.1038/s41684-019-0313-y.

Bresnahan, J. C. (1978) 'An electron-microscopic analysis of axonal alterations following blunt contusion of the spinal cord of the rhesus monkey (Macaca mulatta)', *Journal of the Neurological Sciences*, 37(1–2), pp. 59–82. doi: 10.1016/0022-510X(78)90228-9.

Busch, S. A. *et al.* (2009) 'Overcoming macrophage-mediated axonal dieback following CNS injury', *Journal of Neuroscience*, 29(32), pp. 9967–9976. doi: 10.1523/JNEUROSCI.1151-09.2009.

Chamberlain, K. A. *et al.* (2016) 'Oligodendrocyte regeneration: Its significance in myelin replacement and neuroprotection in multiple sclerosis', *Neuropharmacology*. Elsevier Ltd, pp. 633–643. doi: 10.1016/j.neuropharm.2015.10.010.

Chatzipanteli, K. *et al.* (2000) 'Posttraumatic hypothermia reduces polymorphonuclear leukocyte accumulation following spinal cord injury in rats', *Journal of Neurotrauma*, 17(4), pp. 321–332. doi: 10.1089/neu.2000.17.321.

Cherry, J. D., Olschowka, J. A. and O'Banion, M. K. (2014) 'Neuroinflammation and M2 microglia: The good, the bad, and the inflamed', *Journal of Neuroinflammation*. BioMed Central Ltd. doi: 10.1186/1742-2094-11-98.

Citron, B. A. *et al.* (2000) 'Rapid upregulation of caspase-3 in rat spinal cord after injury: mRNA, protein, and cellular localization correlates with apoptotic cell death', *Experimental Neurology*, 166(2), pp. 213–226. doi: 10.1006/exnr.2000.7523.

Cregg, J. M. *et al.* (2014) 'Functional regeneration beyond the glial scar', *Experimental Neurology*, pp. 197–207. doi: 10.1016/j.expneurol.2013.12.024.

Detloff, M. R. *et al.* (2012) 'Acute and chronic tactile sensory testing after spinal cord injury in rats', *Journal of Visualized Experiments*, (62). doi: 10.3791/3247.

Deuis, J. R., Dvorakova, L. S. and Vetter, I. (2017) 'Methods used to evaluate pain behaviors in rodents', *Frontiers in Molecular Neuroscience*. doi: 10.3389/fnmol.2017.00284.

Duffy, P. *et al.* (2009) 'Rho-associated kinase II (ROCKII) limits axonal growth after trauma within the adult mouse spinal cord', *Journal of Neuroscience*, 29(48), pp. 15266–15276. doi: 10.1523/JNEUROSCI.4650-09.2009.

Ertürk, A. *et al.* (2007) 'Development/Plasticity/Repair Disorganized Microtubules Underlie the Formation of Retraction Bulbs and the Failure of Axonal Regeneration'. doi: 10.1523/JNEUROSCI.0612-07.2007.

Evans, T. A. *et al.* (2014) 'High-resolution intravital imaging reveals that blood-derived macrophages but not resident microglia facilitate secondary axonal dieback in traumatic spinal cord injury', *Experimental Neurology*, 254, pp. 109–120. doi: 10.1016/j.expneurol.2014.01.013.

Faulkner, J. R. *et al.* (2004) 'Reactive Astrocytes Protect Tissue and Preserve Function after Spinal Cord Injury', *Journal of Neuroscience*, 24(9), pp. 2143–2155. doi: 10.1523/JNEUROSCI.3547-03.2004.

Fenrich, K. K. and Rose, P. K. (2011) 'Axons with highly branched terminal regions successfully regenerate across spinal midline transections in the adult cat', *Journal of Comparative Neurology*, 519(16), pp. 3240–3258. doi: 10.1002/cne.22686.

Filous, A. R. *et al.* (2014) 'Entrapment via synaptic-like connections between NG2 proteoglycan + cells and dystrophic axons in the lesion plays a role in regeneration failure after spinal cord injury', *Journal of Neuroscience*, 34(49), pp. 16369–16384. doi: 10.1523/JNEUROSCI.1309-14.2014.

Fitch, M. T. *et al.* (1999) 'Cellular and molecular mechanisms of glial scarring and progressive cavitation: In vivo and in vitro analysis of inflammation-induced secondary injury after CNS trauma', *Journal of Neuroscience*, 19(19), pp. 8182–8198. doi: 10.1523/jneurosci.19-19-08182.1999.

Fleming, J. C. *et al.* (2006) 'The cellular inflammatory response in human spinal cords after injury', *Brain*, 129(12), pp. 3249–3269. doi: 10.1093/brain/awl296.

Fry, E. J. *et al.* (2009) 'Corticospinal tract regeneration after spinal cord injury in receptor protein tyrosine phosphatase sigma deficient mice', *Glia*, p. NA-NA. doi: 10.1002/glia.20934.

Gadani, S. P. *et al.* (2015) 'The Glia-Derived Alarmin IL-33 Orchestrates the Immune Response and Promotes Recovery following CNS Injury', *Neuron*. Cell Press, 85(4), pp. 703–709. doi: 10.1016/j.neuron.2015.01.013.

Geissler, S. A. (2013) 'Rodent Models and Behavioral Outcomes of Cervical Spinal Cord Injury', *Journal of Spine*. OMICS Publishing Group. doi: 10.4172/2165-7939.s4-001.

Gensel, J. C. *et al.* (2006) 'Behavioral and histological characterization of unilateral cervical spinal cord contusion injury in rats', *Journal of Neurotrauma*, 23(1), pp. 36–54. doi: 10.1089/neu.2006.23.36.

Göritz, C. *et al.* (2011) 'A pericyte origin of spinal cord scar tissue', *Science*, 333(6039), pp. 238–242. doi: 10.1126/science.1203165.

Greenhalgh, A. D. and David, S. (2014) 'Differences in the phagocytic response of microglia and peripheral macrophages after spinal cord Injury and its effects on cell death', *Journal of Neuroscience*. Society for Neuroscience, 34(18), pp. 6316–6322. doi: 10.1523/JNEUROSCI.4912-13.2014.

Grossman, S. D., Rosenberg, L. J. and Wrathall, J. R. (2001) 'Temporal-spatial pattern of acute neuronal and glial loss after spinal cord contusion', *Experimental Neurology*, 168(2), pp. 273–282. doi: 10.1006/exnr.2001.7628.

Gwak, Y. S. *et al.* (2012) 'Spatial and temporal activation of spinal glial cells: Role of gliopathy in central

neuropathic pain following spinal cord injury in rats', *Experimental Neurology*, 234(2), pp. 362–372. doi: 10.1016/j.expneurol.2011.10.010.

Hensch, T. K. (2004) 'CRITICAL PERIOD REGULATION', *Annual Review of Neuroscience*. Annual Reviews, 27(1), pp. 549–579. doi: 10.1146/annurev.neuro.27.070203.144327.

Hill, C. E. (2017) 'A view from the ending: Axonal dieback and regeneration following SCI', *Neuroscience Letters*. Elsevier Ireland Ltd, pp. 11–24. doi: 10.1016/j.neulet.2016.11.002.

Horn, K. P. *et al.* (2008) 'Another barrier to regeneration in the CNS: Activated macrophages induce extensive retraction of dystrophic axons through direct physical interactions', *Journal of Neuroscience*, 28(38), pp. 9330–9341. doi: 10.1523/JNEUROSCI.2488-08.2008.

Inman, D. M. and Steward, O. (2003) 'Ascending sensory, but not other long-tract axons, regenerate into the connective tissue matrix that forms at the site of a spinal cord injury in mice', *The Journal of Comparative Neurology*, 462(4), pp. 431–449. doi: 10.1002/cne.10768.

Jones, L. L., Margolis, R. U. and Tuszynski, M. H. (2003) 'The chondroitin sulfate proteoglycans neurocan, brevican, phosphacan, and versican are differentially regulated following spinal cord injury', *Experimental Neurology*, 182(2), pp. 399–411. doi: 10.1016/S0014-4886(03)00087-6.

Karus, M. *et al.* (2016) 'Regulation of oligodendrocyte precursor maintenance by chondroitin sulphate glycosaminoglycans', *GLIA*, 64(2), pp. 270–286. doi: 10.1002/glia.22928.

Kawabata, H. *et al.* (2010) 'High mobility group box 1 is upregulated after spinal cord injury and is associated with neuronal cell apoptosis', *Spine*, 35(11), pp. 1109–1115. doi: 10.1097/BRS.0b013e3181bd14b6.

Keirstead, H. S., Levine, J. M. and Blakemore, W. F. (1998) 'Response of the oligodendrocyte progenitor cell population (Defined by NG2 labelling) to demyelination of the adult spinal cord', *GLIA*, 22(2), pp. 161–170. doi: 10.1002/(SICI)1098-1136(199802)22:2<161::AID-GLIA7>3.0.CO;2-A.

Kigerl, K. A. *et al.* (2009) 'Identification of two distinct macrophage subsets with divergent effects causing either neurotoxicity or regeneration in the injured mouse spinal cord', *Journal of Neuroscience*, 29(43), pp. 13435–13444. doi: 10.1523/JNEUROSCI.3257-09.2009.

Kilpeläinen, I. *et al.* (2000) 'Heparin-binding growth-associated molecule contains two heparin-binding β-sheet domains that are homologous to the thrombospondin type I repeat', *Journal of Biological Chemistry*, 275(18), pp. 13564–13570. doi: 10.1074/jbc.275.18.13564.

Kuboyama, K. *et al.* (2017) 'Protamine neutralizes chondroitin sulfate proteoglycan-mediated inhibition of oligodendrocyte differentiation', *PLoS ONE*. Public Library of Science, 12(12). doi: 10.1371/journal.pone.0189164.

Kucharova, K. and Stallcup, W. B. (2015) 'NG2-proteoglycan-dependent contributions of oligodendrocyte progenitors and myeloid cells to myelin damage and repair', *Journal of Neuroinflammation*. BioMed Central Ltd., 12(1). doi: 10.1186/s12974-015-0385-6.

Kwok, J. C. F. *et al.* (2011) 'Extracellular matrix and perineuronal nets in CNS repair', *Developmental Neurobiology*, 71(11), pp. 1073–1089. doi: 10.1002/dneu.20974.

Kwon, B. K., Hillyer, J. and Tetzlaff, W. (2010) 'Translational research in spinal cord injury: A survey of opinion from the SCI community', *Journal of Neurotrauma*, 27(1), pp. 21–33. doi: 10.1089/neu.2009.1048.

Kwon, B. K., Oxland, T. R. and Tetzlaff, W. (2002) 'Animal models used in spinal cord regeneration research', *Spine*, 27(14), pp. 1504–1510. doi: 10.1097/00007632-200207150-00005.

Laitinen, T. *et al.* (2010) 'Diffusion tensor MRI of axonal plasticity in the rat hippocampus', *NeuroImage*, 51(2), pp. 521–530. doi: 10.1016/j.neuroimage.2010.02.077.

Lang, B. T. *et al.* (2015) 'Modulation of the proteoglycan receptor PTPσ promotes recovery after spinal cord injury', *Nature*, 518(7539), pp. 404–408. doi: 10.1038/nature13974.

Lee, J. H. T. *et al.* (2012) 'A Contusive Model of Unilateral Cervical Spinal Cord Injury Using the Infinite Horizon Impactor', *Journal of Visualized Experiments*, (65). doi: 10.3791/3313.

Lemons, M. L. *et al.* (2003) 'Intact aggrecan and chondroitin sulfate-depleted aggrecan core glycoprotein inhibit axon growth in the adult rat spinal cord', *Experimental Neurology*, 184(2), pp. 981–990. doi: 10.1016/S0014-4886(03)00383-2.

Li, Y.-S. S. *et al.* (1990) 'Cloning and expression of a developmentally regulated protein that induces mitogenic and neurite outgrowth activity', *Science*, 250(4988), pp. 1690–1694. doi: 10.1126/science.2270483.

Li, Y., Field, P. M. and Raisman, G. (1999) 'Death of oligodendrocytes and microglial phagocytosis of myelin precede immigration of Schwann cells into the spinal cord', *Journal of Neurocytology*, 28(4–5), pp. 417–427. doi: 10.1023/A:1007026001189.

Liu, X. Z. *et al.* (1997) 'Neuronal and glial apoptosis after traumatic spinal cord injury', *Journal of Neuroscience*. Society for Neuroscience, 17(14), pp. 5395–5406. doi: 10.1523/JNEUROSCI.17-14-05395.1997.

Luo, F. *et al.* (2018) 'Modulation of proteoglycan receptor PTPσ enhances MMP-2 activity to promote recovery from multiple sclerosis', *Nature Communications*. Nature Publishing Group, 9(1). doi: 10.1038/s41467-018-06505-6.

Lytle, J. M. *et al.* (2009) 'NG2 cell response in the CNP-EGFP mouse after contusive spinal cord injury', *GLIA*, 57(3), pp. 270–285. doi: 10.1002/glia.20755.

Margolis, R. K. and Margolis, R. U. (1993) 'Nervous tissue proteoglycans', *Experientia*, pp. 429–446. doi: 10.1007/BF01923587.

McTigue, D. M., Tripathi, R. and Wei, P. (2006) 'NG2 colocalizes with axons and is expressed by a mixed cell population in spinal cord lesions', *Journal of Neuropathology and Experimental Neurology*, 65(4), pp. 406–420. doi: 10.1097/01.jnen.0000218447.32320.52.

McTigue, D. M., Wei, P. and Stokes, B. T. (2001) 'Proliferation of NG2-positive cells and altered oligodendrocyte numbers in the contused rat spinal cord', *Journal of Neuroscience*, 21(10), pp. 3392–3400. doi: 10.1523/jneurosci.21-10-03392.2001.

Meletis, K. *et al.* (2008) 'Spinal cord injury reveals multilineage differentiation of ependymal cells', *PLoS Biology*, 6(7), pp. 1494–1507. doi: 10.1371/journal.pbio.0060182.

Merenmies, J. and Rauvala, H. (1990) 'Molecular cloning of the 18-kDa growth-associated protein of developing brain', *Journal of Biological Chemistry*, 265(28), pp. 16721–16724. Available at: http://www.jbc.org/ (Accessed: 29 November 2019).

Milev, P. *et al.* (1998) 'High Affinity Binding and Overlapping Localization of Neurocan and Phosphacan/Protein-tyrosine Phosphatase-ζ/β with Tenascin-R, Amphoterin, and the Heparin-binding Growth-associated Molecule', *Journal of Biological Chemistry*, 273(12), pp. 6998–7005. doi: 10.1074/jbc.273.12.6998.

Muradov, J. M., Ewan, E. E. and Hagg, T. (2013) 'Dorsal column sensory axons degenerate due to impaired microvascular perfusion after spinal cord injury in rats', *Experimental Neurology*, 249, pp. 59–73. doi: 10.1016/j.expneurol.2013.08.009.

Nashmi, R. and Fehlings, M. G. (2001) 'Changes in axonal physiology and morphology after chronic compressive injury of the rat thoracic spinal cord', *Neuroscience*, 104(1), pp. 235–251. doi: 10.1016/S0306-4522(01)00009-4.

Nishiyama, A. *et al.* (2002) 'Identity, distribution, and development of polydendrocytes: NG2-expressing glial cells', *Journal of Neurocytology*, pp. 437–455. doi: 10.1023/A:1025783412651.

NSCISC (2018) *2018 Annual Report-Complete Public Version Spinal Cord Injury Model Systems*. Birmingham. Available at: https://www.nscisc.uab.edu/public/2018 Annual Report - Complete Public Version.pdf (Accessed: 19 November 2019).

Pasterkamp, R. J. *et al.* (1999) 'Expression of the gene encoding the chemorepellent semaphorin III is induced in the fibroblast component of neural scar tissue formed following injuries of adult but not neonatal CNS', *Molecular and Cellular Neurosciences*. Academic Press Inc., 13(2), pp. 143–166. doi: 10.1006/mcne.1999.0738.

Paveliev, M. *et al.* (2016) 'HB-GAM (pleiotrophin) reverses inhibition of neural regeneration by the CNS extracellular matrix', *Scientific Reports*. Nature Publishing Group, 6. doi: 10.1038/srep33916.

Pavlov, I. *et al.* (2002) 'Role of heparin-binding growth-associated molecule (HB-GAM) in hippocampal LTP and spatial learning revealed by studies on overexpressing and knockout mice', *Molecular and Cellular Neuroscience*. Academic Press Inc., 20(2), pp. 330–342. doi: 10.1006/mcne.2002.1104.

Pendleton, J. C. *et al.* (2013) 'Chondroitin sulfate proteoglycans inhibit oligodendrocyte myelination through PTPσ'. doi: 10.1016/j.expneurol.2013.04.003.

Plunet, W. T. *et al.* (2008) 'Dietary restriction started after spinal cord injury improves functional recovery', *Experimental Neurology*, 213(1), pp. 28–35. doi: 10.1016/j.expneurol.2008.04.011.

Raulo, E. *et al.* (1992) *THE JOURNAL OF BIOLOGICAL CHEMISTRY Secretion and Biological Activities of Heparin-binding Growth-associated Molecule NEURITE OUTGROWTH-PROMOTING AND MITOGENIC ACTIONS OF THE RECOMBINANT AND TISSUE-DERIVED PROTEIN**.

Rauvala, H. (1989) 'An 18-kd heparin-binding protein of developing brain that is distinct from fibroblast growth factors.', *The EMBO Journal*. Wiley, 8(10), pp. 2933–2941. doi: 10.1002/j.1460-2075.1989.tb08443.x.

Rauvala, H. *et al.* (1994) 'Expression of HB-GAM (heparin-binding growth-associated molecules) in the pathways of developing axonal processes in vivo and neurite outgrowth in vitro induced by HB-GAM', *Developmental Brain Research*, 79(2), pp. 157–176. doi: 10.1016/0165-3806(94)90121-X.

Rauvala, H. *et al.* (2000) 'Heparin-binding proteins HB-GAM (pleiotrophin) and amphoterin in the regulation of cell motility', *Matrix Biology*. Elsevier, pp. 377–387. doi: 10.1016/S0945-053X(00)00084-6.

Rauvala, H. *et al.* (2017) 'Inhibition and enhancement of neural regeneration by chondroitin sulfate proteoglycans', *Neural Regeneration Research*. Medknow Publications, pp. 687–691. doi: 10.4103/1673-5374.206630.

Rodriguez, J. P. *et al.* (2014) 'Abrogation of β-Catenin signaling in oligodendrocyte precursor cells reduces glial scarring and promotes axon regeneration after CNS injury', *Journal of Neuroscience*, 34(31), pp. 10285–10297. doi: 10.1523/JNEUROSCI.4915-13.2014.

Roitbak, T. and Syková, E. (1999) 'Diffusion barriers evoked in the rat cortex by reactive astrogliosis', *GLIA*, 28(1), pp. 40–48. doi: 10.1002/(SICI)1098-1136(199910)28:1<40::AID-GLIA5>3.0.CO;2-6.

Rolls, A., Shechter, R. and Schwartz, M. (2009) 'The bright side of the glial scar in CNS repair', *Nature Reviews Neuroscience*, 10(3), pp. 235–241. doi: 10.1038/nrn2591.

Sandler, A. N. and Tator, C. H. (1976) 'Review of the effect of spinal cord trauma on the vessels and blood flow in the spinal cord', *Journal of Neurosurgery*, 45(6), pp. 638–646. doi: 10.3171/jns.1976.45.6.0638.

Sato, Y. *et al.* (2008) 'A highly sulfated chondroitin sulfate preparation, CS-E, prevents excitatory amino acid-induced neuronal cell death', *Journal of Neurochemistry*, 104(6), pp. 1565–1576. doi: 10.1111/j.1471-4159.2007.05107.x.

Savaskan, N. E. *et al.* (2009) 'High resolution neurochemical gold staining method for myelin in peripheral and central nervous system at the light- and electron-microscopic level', *Cell and Tissue Research*, 337(2), pp. 213–221. doi: 10.1007/s00441-009-0815-9.

Seibenhener, M. L. and Wooten, M. C. (2015) 'Use of the Open Field Maze to Measure Locomotor and Anxiety-like Behavior in Mice', *Journal of Visualized Experiments*, (96). doi: 10.3791/52434.

Sharif-Alhoseini, M. *et al.* (2017) 'Animal models of spinal cord injury: A systematic review', *Spinal Cord*. Nature Publishing Group, pp. 714–721. doi: 10.1038/sc.2016.187.

Shechter, R. *et al.* (2009) 'Infiltrating blood-derived macrophages are vital cells playing an anti-inflammatory role in recovery from spinal cord injury in mice', *PLoS Medicine*. Edited by M. B. Graeber, 6(7), p. e1000113. doi: 10.1371/journal.pmed.1000113.

Shen, Y. *et al.* (2009) 'PTP Is a Receptor for Chondroitin Sulfate Proteoglycan, an Inhibitor of Neural Regeneration', *Science*, 326(5952), pp. 592–596. doi: 10.1126/science.1178310.

Silver, J. and Miller, J. H. (2004) 'Regeneration beyond the glial scar', *Nature Reviews Neuroscience*. European Association for Cardio-Thoracic Surgery, pp. 146–156. doi: 10.1038/nrn1326.

Singh, A. *et al.* (2014) 'Global Prevalence and incidence of traumatic spinal cord injury', *Clinical Epidemiology*. Dove Medical Press Ltd, pp. 309–331. doi: 10.2147/CLEP.S68889.

Snow, D. M. *et al.* (1990) 'Sulfated proteoglycans in astroglial barriers inhibit neurite outgrowth in vitro', *Experimental Neurology*, 109(1), pp. 111–130. doi: 10.1016/S0014-4886(05)80013-5.

Sobel, R. A. and Ahmed, A. S. (2001) 'White Matter Extracellular Matrix Chondroitin Sulfate/Dermatan Sulfate Proteoglycans in Multiple Sclerosis', *Journal of Neuropathology & Experimental Neurology*, 60(12), pp. 1198–1207. doi: 10.1093/jnen/60.12.1198.

Soblosky, J. S., Song, J.-H. and Dinh, D. H. (2001) *Graded unilateral cervical spinal cord injury in the rat: evaluation of forelimb recovery and histological effects*, *Behavioural Brain Research*. Available at: www.elsevier.com/locate/bbr (Accessed: 26 September 2019).

Soderblom, C. *et al.* (2013) 'Perivascular fibroblasts form the fibrotic scar after contusive spinal cord injury', *Journal of Neuroscience*, 33(34), pp. 13882–13887. doi: 10.1523/JNEUROSCI.2524-13.2013.

Stirling, D. P. *et al.* (2009) 'Depletion of Ly6G/Gr-1 leukocytes after spinal cord injury in mice alters wound healing and worsens neurological outcome', *Journal of Neuroscience*, 29(3), pp. 753–764. doi: 10.1523/JNEUROSCI.4918-08.2009.

Streijger, F. *et al.* (2013) 'Characterization of a Cervical Spinal Cord Hemicontusion Injury in Mice Using the Infinite Horizon Impactor', *Journal of Neurotrauma*, 30(10), pp. 869–883. doi: 10.1089/neu.2012.2405.

Sugahara, K. and Mikami, T. (2007) 'Chondroitin/dermatan sulfate in the central nervous system', *Current Opinion in Structural Biology*, pp. 536–545. doi: 10.1016/j.sbi.2007.08.015.

Sun, D. *et al.* (2010) 'Structural remodeling of fibrous astrocytes after axonal injury', *Journal of Neuroscience*, 30(42), pp. 14008–14019. doi: 10.1523/JNEUROSCI.3605-10.2010.

Takeda, A. *et al.* (1995) 'Induction of heparin-binding growth-associated molecule expression in reactive astrocytes following hippocampal neuronal injury', *Neuroscience*, 68(1), pp. 57–64. doi: 10.1016/0306-4522(95)00110-5.

Tang, X., Davies, J. E. and Davies, S. J. A. (2003) 'Changes in distribution, cell associations, and protein expression levels of NG2, neurocan, phosphacan, brevican, versican V2, and tenascin-C during acute to chronic maturation of spinal cord scar tissue', *Journal of Neuroscience Research*, 71(3), pp. 427–444. doi: 10.1002/jnr.10523.

Tattersall, R. and Turner, B. (2000) 'Brown-Séquard and his syndrome', *Lancet*, pp. 61–63. doi: 10.1016/S0140-6736(00)02441-7.

Tom, V. J. *et al.* (2004) 'Studies on the development and behavior of the dystrophic growth cone, the hallmark of regeneration failure, in an in vitro model of the glial scar and after spinal cord injury.', *J. Neurosci.* Society for Neuroscience, 23(2), pp. 493–502. doi: 20026637.

Tran, A. P., Warren, P. M. and Silver, J. (2018) 'The biology of regeneration failure and success after spinal cord injury', *Physiological Reviews*. American Physiological Society, pp. 881–917. doi: 10.1152/physrev.00017.2017.

Treede, R. D. and Magerl, W. (2000) 'Multiple mechanisms of secondary hyperalgesia', *Progress in Brain Research*. Elsevier, 129, pp. 331–341. doi: 10.1016/S0079-6123(00)29025-0.

Trivedi, A., Olivas, A. D. and Noble-Haeusslein, L. J. (2006) 'Inflammation and spinal cord injury: Infiltrating leukocytes as determinants of injury and repair processes', *Clinical Neuroscience Research*, 6(5), pp. 283–292. doi: 10.1016/j.cnr.2006.09.007.

Vandamme, T. (2014) 'Use of rodents as models of human diseases', *Journal of Pharmacy and Bioallied Sciences*. Medknow Publications, pp. 2–9. doi: 10.4103/0975-7406.124301.

Vogelaar, C. F. and Estrada, V. (2016) 'Experimental Spinal Cord Injury Models in Rodents: Anatomical Correlations and Assessment of Motor Recovery', in *Recovery of Motor Function Following Spinal Cord Injury*. InTech. doi: 10.5772/62947.

Voříšek, I. *et al.* (2002) 'Water ADC, extracellular space volume, and tortuosity in the rat cortex after traumatic injury', *Magnetic Resonance in Medicine*, 48(6), pp. 994–1003. doi: 10.1002/mrm.10305.

Wang, Y.-T. *et al.* (2004) 'Upregulation of heparin-binding growth-associated molecule after spinal cord injury in adult rats.', *Acta pharmacologica Sinica*, 25(5), pp. 611–6. Available at: http://www.ncbi.nlm.nih.gov/pubmed/15132827 (Accessed: 28 November 2019).

Wanner, I. B. *et al.* (2008) 'A new *in vitro* model of the glial scar inhibits axon growth', *Glia*, 56(15), pp. 1691–1709. doi: 10.1002/glia.20721.

Wanner, I. B. *et al.* (2013) 'Glial scar borders are formed by newly proliferated, elongated astrocytes that interact to corral inflammatory and fibrotic cells via STAT3-dependent mechanisms after spinal cord injury', *Journal of Neuroscience*, 33(31), pp. 12870–12886. doi: 10.1523/JNEUROSCI.2121-13.2013.

World Health Organization (2019) *Spinal cord injury*. Available at: https://www.who.int/news-room/fact-sheets/detail/spinal-cord-injury (Accessed: 19 November 2019).

Wu, D. *et al.* (2005) 'Different expression of macrophages and microglia in rat spinal cord contusion injury model at morphological and regional levels.', *Acta medica Okayama*, 59(4), pp. 121–7. doi: 10.18926/AMO/31950.

Xu, B. *et al.* (2015) 'Role of CSPG receptor LAR phosphatase in restricting axon regeneration after CNS injury', *Neurobiology of Disease*, 73, pp. 36–48. doi: 10.1016/j.nbd.2014.08.030.

Xu, K. *et al.* (1999) 'Glial fibrillary acidic protein is necessary for mature astrocytes to react to β-amyloid', *GLIA*, 25(4), pp. 390–403. doi: 10.1002/(SICI)1098-1136(19990215)25:4<390::AID-GLIA8>3.0.CO;2-7.

Yeh, H.-J. *et al.* (1998) 'Upregulation of Pleiotrophin Gene Expression in Developing Microvasculature, Macrophages, and Astrocytes after Acute Ischemic Brain Injury', *The Journal of Neuroscience*, 18(10), pp. 3699–3707. doi: 10.1523/JNEUROSCI.18-10-03699.1998.

Zhu, X., Hill, R. A. and Nishiyama, A. (2008) 'NG2 cells generate oligodendrocytes and gray matter astrocytes in the spinal cord', *Neuron Glia Biology*, 4(1), pp. 19–26. doi: 10.1017/S1740925X09000015.